UNIVERSITY OF OKLAHOMA

# RESEARCH INSTITUTE

PROJECT 52

# FINAL REPORT

to

OFFICE OF NAVAL RESEARCH

Project Number NR 072-221/9-21-49
Contract Number N9 onr 97700

December 31, 1952

FINAL REPORT

# RESEARCH ON RADIATION TRANSIENTS IN GAS DISCHARGES

December 31, 1952

Project Number NR 072-221/9-21-49

Contract Number N9 onr 97700

BY

Richard G. Fowler
William R. Atkinson
Beryl E. Clotfelter
Robert J. Lee

University of Oklahoma
Norman, Oklahoma

ACKNOWLEDGMENT

The authors are grateful to Messrs. Thomas R. Coleman, Walter D. Compton, Alfred Kleider, Luther W. Marks, and Howard C. Rose for their gratuitous assistance on the studies identifying the contact surface, of reflected luminous fronts, Doppler effect, the radiation law in T-tubes, and the radiation law in shock tubes respectively. Details of this work are embodied in M.S. theses by these gentlemen deposited in the Graduate College of the University of Oklahoma.

They are deeply indebted to Professor Otto Laporte of the University of Michigan for his valuable suggestions on the fluid flow aspects of the discharge, and to Professor Leonard Loeb of the University of California for his assistance in interpreting the gaseous electronic phenomena observed.

TABLE OF CONTENTS

ABSTRACT

Suitably arranged low pressure spark discharges are followed by an expansion of the ion cloud which offers a clue to the mechanisms in the spark discharge. The expansion is accompanied by many peculiar and complex phenomena of which a partial understanding has been reached. The expansion is violent and is generally preceded in the surrounding gas by a very strong shock wave which frequently exhibits an intense luminosity that is largely intrinsic. During the expansion the reservior of internal energy in the ion cloud maintains the ionization and is converted into radiation over an extended time interval according to the processes present in a stellar atmosphere, thus prolonging the discharge well beyond the interval which electric circuit calculations of current decay would indicate. It seems certain that a complete understanding of the spark discharge will not be achieved until the auxiliary mechanical or acoustical effects have been taken into account.

# CHAPTER I

## HISTORICAL INTRODUCTION

Many studies of low pressure spark discharges have been made for an equally diverse number of reasons. The transient state of the discharge has long been recognized as an interval in which nature reveals the character of her processes more completely than at any other time. In 1835 Wheatstone determined with a rotating mirror and an induction coil that the luminosity in the spark moved as a front down the tube, traveling with a speed of upwards of $8 \times 10^7$ cm/sec. Von Zahn (1) could detect no Doppler shift in these fronts and concluded that there was no mass motion of the gas. J. J. Thomson (2) devised an ingenious rotating mirror method for measuring the time interval of passage of the luminosity between two points of the discharge tube, finding thus that it moved with one-third the speed of light and was independent of the nature of the gas and of the electrodes.

Beams (3) made improvements in the rotating mirror technique and demonstrated that the luminous fronts did indeed have velocities of the order observed by Thomson. He found that the fronts traveled from the free potential electrode to ground, regardless of the sign of the charge on the free electrode. He found that this speed was also independent of polarity, increased with decreasing pressure, and increased somewhat with increasing potential difference. Altering the composition of the tube wall made a definite change in the velocity. Further experiments (4) with a cathode ray oscillograph showed that some sort of electrical disturbance was indeed propagated through the tube with speeds nearly identical with those of the luminous fronts. No evidence was obtained that the luminosity wave was co-spatial with the potential wave. A reflected wave was observed which traveled at higher speed than the initial wave, probably because of the ionized gas through which it was returning.

Investigations of the mechanisms for the initiation of spark discharges have been reviewed recently by Loeb (5). It has been found that the Townsend theory of the initiation of the discharge is not adequate at high pressures. It is proposed that the photoionization of the gas produced in the vicinity of the discharge instigating electron is a primary process in the development of a streamer of ionization which quickly connects cathode to anode, and this is regarded as the mechanism of the disturbances observed by the workers cited above. The Townsend process requires about $10^{-5}$ seconds for initiation. The photo-ionization process requires several orders of magnitude less time, operating as it does by the agency of electromagnetic radiation.

A new avenue of approach was opened when Rayleigh (6) observed that the luminosity during a low pressure spark was not confined to the path directly joining the electrodes as in the glow discharge, but invaded branch paths regardless of the electrical character of their termini. This escape of luminosity from the electrodeless discharge was a well-known effect to workers with that discharge, but had always been set down to leakage currents down grounded paths of the vacuum circuit. Smear photographs taken with a rotating mirror, used by Rayleigh as a wave speed camera, showed that the velocity of advance of the escaping luminosity was small compared with the velocities measured by the investigators of spark streamers. Assuming that the excitation acts preceding radiation of the luminosity had been accomplished completely in the discharge path proper and then ejected as excited but unionized systems in a livid mass into the side tube by the large pressures created by the discharge, Rayleigh concluded that the relaxation lifetime of excited states was anomalously long. An estimate of this lifetime for hydrogen placed it at $10^{-5}$ seconds.

This value being incompatible with the well-known lifetimes of excited states, Zanstra (7) suggested that the luminosity was the result of recombination among the ejected ions.

Lee and Fowler ( 8 ), however, using an electrodeless discharge apparatus essentially similar to that of Rayleigh, showed that what had appeared to be an ejected tongue of luminous gas in the Rayleigh experiments was in reality a succession of unresolved luminous fronts, resulting from oscillatory capacitor discharge, and moving down the branch tube. This rendered the hypothesis of Zanstra insufficient, since the luminosity, if created in the main discharge and expelled from it, should be a monotonically decreasing function of both time and position along the side tube. Fronts of luminosity in the side tube indicate excitation processes which continue without the aid of the electric fields in the main discharge.

Lee and Fowler also showed that the fronts will pass through charged or grounded grids, and between charged plates, without apparent alteration. Presence of a magnetic field at right angles to the direction of motion of the front deflected a charge to the plates even though they were initially uncharged. It was concluded that the fronts had a plasma composition, and that the ions in the front were in motion in the direction of propagation of the front. This deviation from the conclusions of Von Zahn indicates a definite difference between the phenomena.

Goldstein and Fowler ( 9 ) produced fronts of the same character as those above by discharging a 12 $\mu$fd condenser abruptly through a straight discharge tube 15 cm long having electrodes in either end and a side arm in the middle. It was found that the fronts could be produced in any kind of gas, and that the velocity of propagation was intimately related to the molecular weight of the gas, being greatest in hydrogen, least in argon. Gases tested were hydrogen, helium, nitrogen, neon, and argon. The velocity of propagation, although determined only roughly, was found to lie slightly above the acoustical range and to increase with decreasing pressure and with increasing potential. These results led to the conclusion that the factor governing the velocity of the front was energy per unit mass of gas in the discharge.

When a constriction was placed in the side arm of the discharge tube, a reflected front was observed which traveled with a velocity greater than that of the incident front. This fact was interpreted to mean that the increased temperature of the gas in the tube after the passage of the incident front was the cause of the increased speed. Coupled with the electrically neutral character of the front, the order of magnitude of its velocity, and the effects of molecular weight on velocity, it was hypothesized tentatively that the luminous front was an acoustical pulse wave of great energy.

Clotfelter and Fowler (9) used improved apparatus to establish discharge dependences. Hydrogen was used exclusively. Accuracy of measurement of velocity was still unsatisfactory but the previously observed dependences on pressure and condenser potential were confirmed. The luminous fronts were introduced into tubes of various diameters and it was found that the distance of maximum advance of the front increased with pressure and tube diameter.

Spectroscopic examinations of the discharge were made which hinted at a considerable broadening of the Balmer lines, and showed the Balmer series to break off at $H_\theta$ and an intense continuum to exist beyond this point, terminating at around 3200 $A^o$. This continuum raised once again the possibility of extensive recombination which had been largely abandoned when the luminosity was resolved into fronts rather than jets in the experiments of Lee and Fowler.

The luminosity emitted by gas discharges has also been the subject of a considerable spectroscopic study. The spectrum of hydrogen, with which we were in particular concerned initially, has been studied in many ways. Hydrogen emits both atomic and molecular spectra when suitably excited. Both atom and molecule have continuous and line spectra. Finkelnberg (10) investigated the transition from the sharp and discrete Balmer line spectrum to an atomic continuum in which all the lines had been obliterated by the random

electric fields of the ion cloud (Stark effect). He produced this transition in two discharges of apparently different characteristics, although, by the principle of similarity they may be more alike than at first appears. In the one case he used a 30,000 volt condensed discharge through a 1 mm spark gap immersed in hydrogen of up to 30 atmospheres pressure. In the other he used a 6,000 volt condensed discharge through a large diameter tube at 1 mm pressure. The observed half-widths of the lines of the Balmer series and the pressures of obliteration of the various lines both led to a calculation of local field intensities in good agreement with the work of Von Traubenberg (11) on Stark broadening.

The effects observed by Finkelnberg are integrated properties of the discharge both with respect to time and position, and so give little indication of the excitation and radiation mechanisms.

Craggs and Hopwood (12) utilized the Holtsmark theory of Stark broadening in a fashion similar to Finkelnberg in their study of the expansion of initial spark streamers into full fledged arc columns during the course of a spark discharge. They pointed out that the contours of the broadened lines are just what would be expected of Stark broadening, and cited reasons for believing that the luminosity produced during the spark must be largely contributed by electronic recombination. We have observed these peculiar line contours in our discharges and arrived at the same conclusion: that they constitute the strongest evidence for interpreting the broadening as Stark broadening.

Since the inception of this project Olsen and Huxford (13) have reported their measurements of ion concentrations in photoflash tubes under conditions which parallel our work to a considerable degree. On the assumption that the Holtsmark theory of Stark broadening applies to their apparatus without modification, they have found that the ion concentration in a tube rises and falls in time with a rather large time lag with respect to the rise and fall of

current. They have also found that the continuum is in large measure attributable to bremsstrahlung processes rather than recombination.

## Statement of the Problem

The entire phenomenon described in the historical introduction seemed anomalous with respect to theories of electrical discharges. The duration of the expanding luminosity was too great to be explained as atomic relaxation. The space distribution of the luminosity was often improper to be explained as a recombination of ions produced during the discharge. Accordingly, research was begun to describe the properties and identify the causes of this phenomenon which we have chosen to term the Rayleigh phenomenon. Specifically we proposed to discover (1) the mechanics of the expansion, (2) the steps of energy transfer which lead to the production of excited atomic systems, and (3) the nature of these systems.

## CHAPTER II

## INSTRUMENTATION

1. Wave speed camera.

A six-inch concave rotatable mirror of one meter focal length has been constructed as a high precision wave speed camera for the study of self luminous wave phenomena. Reduction of optical aberrations to a minimum has been accomplished by using a mirror of astronomical quality under conditions which closely approach the paraxial ray approximation. Use of a large object distance (7.6 meters) resulted in increased photographic speed and also extended the usable range of velocities to higher values than could previously be measured with accuracy. An aberration-free focal area about 4 cm wide and centered about the optic axis was available as the mirror image swept across the film. To register pictures entirely in this area, a triggering device was constructed to initiate the spark discharge. A source of infra-red light was directed off the mirror onto a photocell at the epoch appropriate to produce registration of the subsequently created luminous wave. The pulse created by a transit of the infra-red lamp reflection across the photocell face was amplified and delivered to a thyratron in the switching circuit. There was a delay of about 1000 $\mu$secs between trip and registry in the particular switching circuit used, caused by the inertia of the mechanical switch used to initiate the discharge. Circuits for this equipment are given in Figure 1. The operating and constructional characteristics of the mirror are given in Table 1.

The clarity of picture obtained with this wave speed camera made it possible to recognize features of the expansion of luminous gases which had hitherto remained unobserved.

2. Energy storage and the discharge circuit.

Energies of the order of 10 joules at powers of the order of a megawatt

Table 1

Mirror Characteristics

| | |
|---|---|
| Mirror diameter | 6" |
| Focal length | 1 meter |
| Rotation | designed for 60 rps, used hitherto at 30 rps |
| Registration error (mean) | .5 cm from axis |
| Linear sweep speed | 1 cm/23.3 $\mu$ sec. |

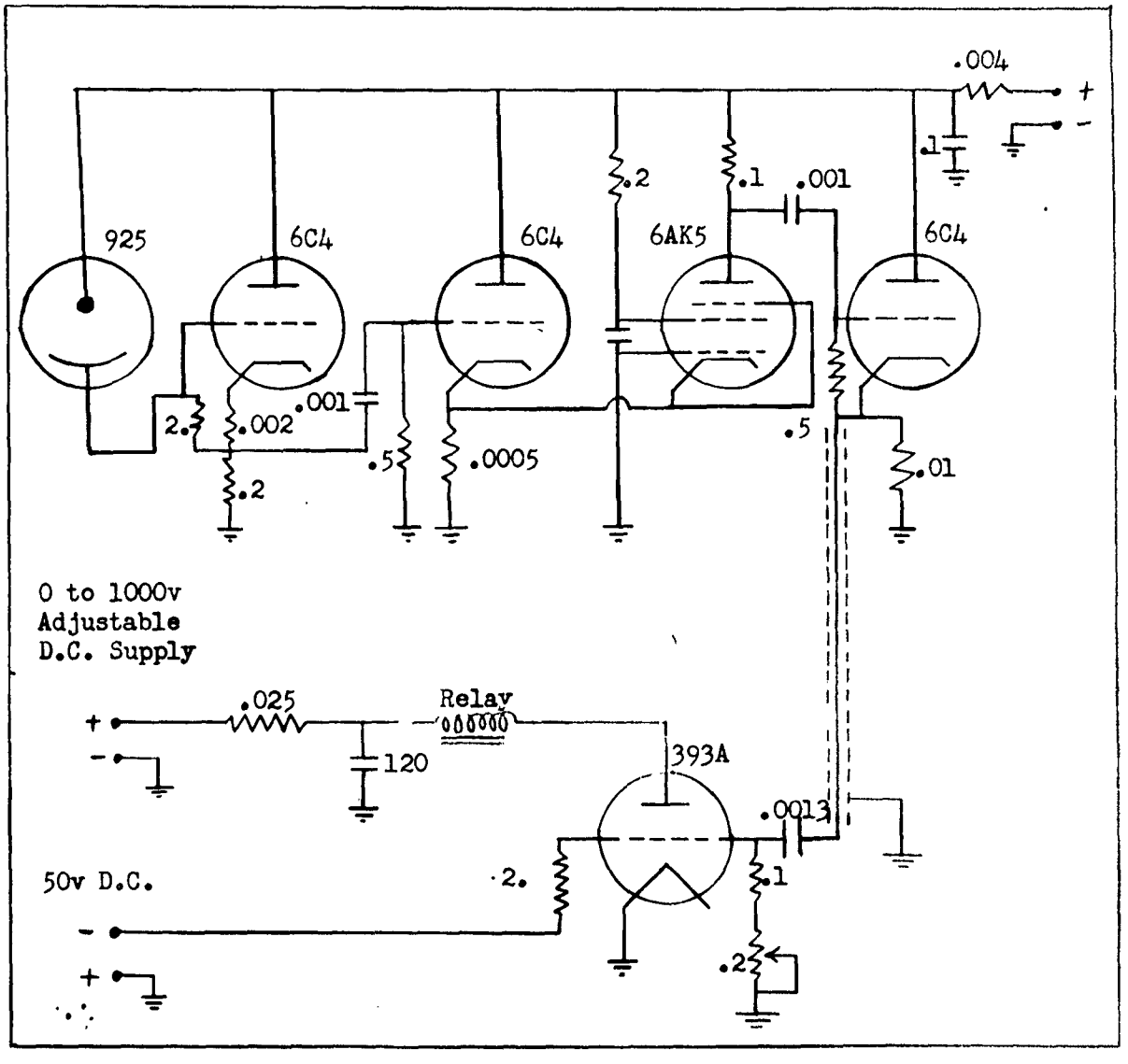


Fig. 1. Mirror synchronized relay circuit for controlling discharge. Capacitances are in microfarads. Resistances are in megohms.

are needed to produce the Rayleigh phenomenon. We have found pyranol-filled capacitors reasonably reliable for this work. When used singly or in parallel they have given long service, with lifetimes in excess of $10^5$ discharges. When used in series they have invariably failed because of an apparent tendency of one capacitor to charge the other to excessive potentials. We have worked with capacitors ranging from 1 to 50 microfarads, charged to potentials ranging from 1000 to 10,000 volts.

The abrupt discharge of these capacitors is frequently accompanied by an intense transient oscillation decaying to zero from the full capacitor potential in about 30 cycles, at a frequency of 30 to 100 megacycles depending on the particular capacitor. This oscillation was unaffected by external circuit constants, and we believe that it must have been a loaded line oscillation of the capacitor foils. To prevent it from entering into the discharge under investigation we introduced a filter into the discharge path in our later work. The filter consisted of the critical damping resistor divided into two portions, with two .1 $\mu$fd bypass capacitors.

The apparent internal series inductances and resistances of several storage capacitors have been checked by a study of their discharge transients. In a similar fashion, the apparent lumped series inductances and resistances of two particular discharge circuits have been estimated. These measurements are given in Table 2.

Table 2

Capacitor Constants

| Capacitor | Capacitance | Internal Inductance | Internal resistance |
|---|---|---|---|
| (a) GE. 14F9 | $5.0 \times 10^{-6}$f | $.36 \times 10^{-6}$h | .035 $\Omega$ |
| (b) West. 1176638 | $1.0 \times 10^{-6}$f | $.36 \times 10^{-6}$h | .18 $\Omega$ |
| (c) GE. 14F63 | $1.0 \times 10^{-6}$f | $.32 \times 10^{-6}$h | .12 $\Omega$ |

Table 2 (continued)

Capacitor Constants

| Capacitor | Capacitance | Internal Inductance | Internal resistance |
|---|---|---|---|
| (d) GE 14F59 | $1.0 \times 10^{-6}$f | $.57 \times 10^{-6}$h | .16Ω |
| (e) GE 26F681 | $1.0 \times 10^{-6}$f | $.35 \times 10^{-6}$h | .26Ω |
| (f) 25-807-2-7 | $12.0 \times 10^{-6}$f | $2.5 \times 10^{-6}$h | .08Ω |

Circuit Constants

| Capacitor | Circuit Inductance | Circuit resistance |
|---|---|---|
| (a) Bank of 12 type (b) above | $1.5 \times 10^{-6}$h | .10 - .15 |
| (b) GE 14F3 | $1.4 \times 10^{-6}$h | |

Damping of the discharge causes a modest reduction in the velocity of the luminous fronts. Since the velocity of the fronts is probably governed by the power expenditure in the discharge, this effect of increased damping is easily understandable. On the assumption that the tube resistance is ohmic, maximum power dissipated in the critically damped case is

$$P_m = \frac{rCV^2}{L} e^{-2} ,$$

where r is the tube resistance, C is the capacitance, V is the initial capacitor potential, and L is the distributed inductance. The maximum power dissipated in the underdamped case is

$$P_m = \frac{rCV^2}{L} e^{-\frac{R}{\omega L} \tan^{-1} \frac{2\omega L}{R}} ,$$

where R is the total distributed resistance of the circuit, and $\omega$ is the angular natural frequency

$$\omega = \sqrt{\frac{1}{LC} - \frac{R^2}{4L^2}} .$$

Since the power in the latter case is always more than that in the former because for all positive real values of $\theta$,

$$\frac{1}{\theta} \tan^{-1} 2\theta \leqslant 2$$

and since the equal sign applies only in the critically damped case, we reach the conclusion that the flow velocities u are related by

$$u_{\max, \text{ critical}} \leqslant u_{\max, \text{ underdamped}} .$$

In operation it has been found desirable to damp the discharge critically using a noninductively wound section of manganin wire. The actual resistances used have been determined by experiment, but agree reasonably well with theory, despite the non-linear behavior of the gas tube which occupies the chief place in the circuit.

Critical damping

| Theoretical | Experimental |
|---|---|
| .70 Ω | .5 - .60 Ω |

The circuit most commonly used was the simple series circuit shown in Fig. 2. Wherever possible the leads of the circuit were run coaxially to mini-

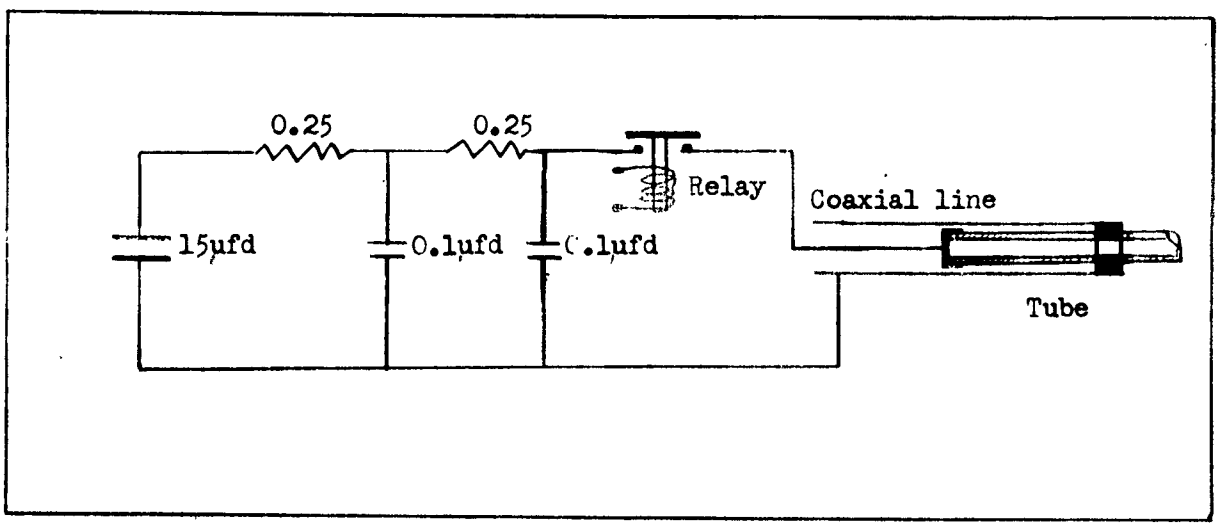


Fig. 2. Typical discharge circuit for exciting the Rayleigh Phenomenon.

mize inductance. An aluminum wall was placed so that it divided the power circuits from the discharge tube to serve as an electrical ground for the system and reduce the reception of stray signals at any electrical detectors used in the tube.

3. Switching.

Our preference in devices for closing of the discharge circuit has been metal-to-metal contact. If this contact were made in a gas, an arc could form between the contacts before they are completely closed, and because of the slowness with which any relay closes, probably would endure throughout the entire discharge which normally lasts only 10 $\mu$sec. Such arcs might impress unwanted characteristics upon the discharge under observation. Actually, however, they were probably rarely encountered in our work. If the discharge tube is itself carefully deionized and leakage currents paralleling it are minimized, there should be no breakdown of the gas between the switch contacts during closure because the distribution of the electrostatic potential difference would give a less-than-breakdown value across the switch. Whenever the research problem necessitates leakage paths around or through the discharge tube, vacuum switches are the only feasible kind. We have employed both arrangements and both types of switching with reasonable success.

An ideal switch would be capable of standing off potentials of the order of $10^4$ volts, extremely quick in closing (100-1000 $\mu$sec), would close and remain closed during the discharge, and would have contacts capable of carrying five or ten thousand amperes. We found that in practice the contacts frequently reopen immediately after closure. This, we concluded, was caused by the stationary electrode moving away under impact compression rather than by bouncing of the moving electrode. We found that switches from which reopening had been eliminated (by facing the contacts, by minimizing the mass of the moving electrode, and by increasing the holding force acting on the armature)

closed without arcing up to capacitor potentials of 3000 volts, but appeared to break down above this. Since the maximum discharge current increases linearly with the capacitor potential, we believe that this critical point was one at which the fall in potential across the contact impedance exceeded the breakdown potential of the gas, and hence precipitated a gas discharge around the point of contact. We have found that a hydrogen atmosphere around our switch was beneficial in preventing oxidation during this period of arcing.

Thyratron or ignitron switching has been considered but was not used because of the excessive current demands which would require very large tubes and probably increase the circuit inductance to an undesirable degree.

A liquid-mercury-in-vacuum switch was constructed according to what seemed a very promising design. A pool of mercury rolled to join two separated electrode pools when the switch was tilted. A liquid air trap was built directly over the contacts to maintain the vacuum to a high degree. After two or three cycles the entire switch exploded, apparently from internal forces in the current-bearing liquid mercury column.

4. Tube construction.

We have investigated in some detail the effect on the discharge of tube construction. Composition of the tube walls, shape and size of the tube, location, composition and spacing of the electrodes have been varied over wide limits.

Composition of the electrodes has not been investigated to a full understanding, although certain facts are clear. Many of the considerations under which suitable material would be chosen for such devices as Edgerton lamps or Geissler tubes do not seem to apply here. Aluminum electrodes were used initially because it was felt that low work function material would be desirable, and that in general conditions which reduced sputtering should be favored. Two peculiarities were noted. When pure aluminum was used, the

discharge tube would "poison", so that after each discharge the starting potential increased until finally it became impossible to obtain a discharge. The effect became more prominent as the purity was increased, and was ascribed to the formation of a non-conducting layer on the aluminum, probably an oxide layer. A second effect was observed at low pressures. Below 1 mm Hg the spectrum of aluminum was very prominent in the main tube when aluminum electrodes were used. When nickel was later substituted for aluminum, the discharge was not producible much below 1 mm pressure (in hydrogen), although it had been operated successfully down to .2 mm with aluminum electrodes. It seems certain that these are related facts, and that the aluminum vapor, whose spectrum was observed, substituted for hydrogen in the operation of the discharge at low pressures.

The most desirable feature which good electrode materials should possess for use in studying these low pressure spark discharges seems to be low volatility, although there are certainly other unknown factors which govern the choice. In a brief survey of materials in which the only criterion was whether the spectrum of the metal could be observed, the following order was found among elements tested, best to worst: nickel, copper, tungsten, aluminum. Nickel vapor was almost unobservable in the discharges in which nickel was used. It is probable that the lack of success with tungsten can be attributed to the small size of the electrodes used (1/10 inch) and the consequently enormous current densities at the electrode.

At constant spacing, the location of the electrodes relative to the side arm where the fronts are observed was found to have little effect on the fronts as long as the side arm lay between the electrodes. The velocity was slightly less when the side arm was very near to either electrode.

Separation of the electrodes had only a slight influence on the front behavior over a range from .7 cm to 17 cm. As would be expected, the damping

on the circuit increased as the separation was increased. The fraction of the energy of the capacitor which was absorbed by the tube during a single oscillation increased as the tube was lengthened. At the same time, the volume of gas over which the energy was distributed increased. Hence, the velocity of the fronts might be expected to pass through a maximum at some electrode separation, the value of which should depend on initial gas pressure and tube diameter. Such a maximum was indeed found at 9 cm separation in air, between 1 and 3 mm pressure, in a tube with 12.5 mm inside diameter.

The shape of the discharge tube had a small influence on the maximum velocity of the fronts but a large influence on the character of the postfrontal luminosity. Two principal tube styles have been examined, the "T" tube and the "shock" tube. The "T" was an early paraphrase of the Rayleigh apparatus, where the main discharge was at right angles to the expansion chamber. Although most of our investigations have been conducted with it, it is not as well adapted to investigations which might have theoretical support as is the "shock" tube, in which the main discharge is along a portion of the same column that the expansion chamber occupies. The three styles of tubes which have been studied are shown in Figure 3.

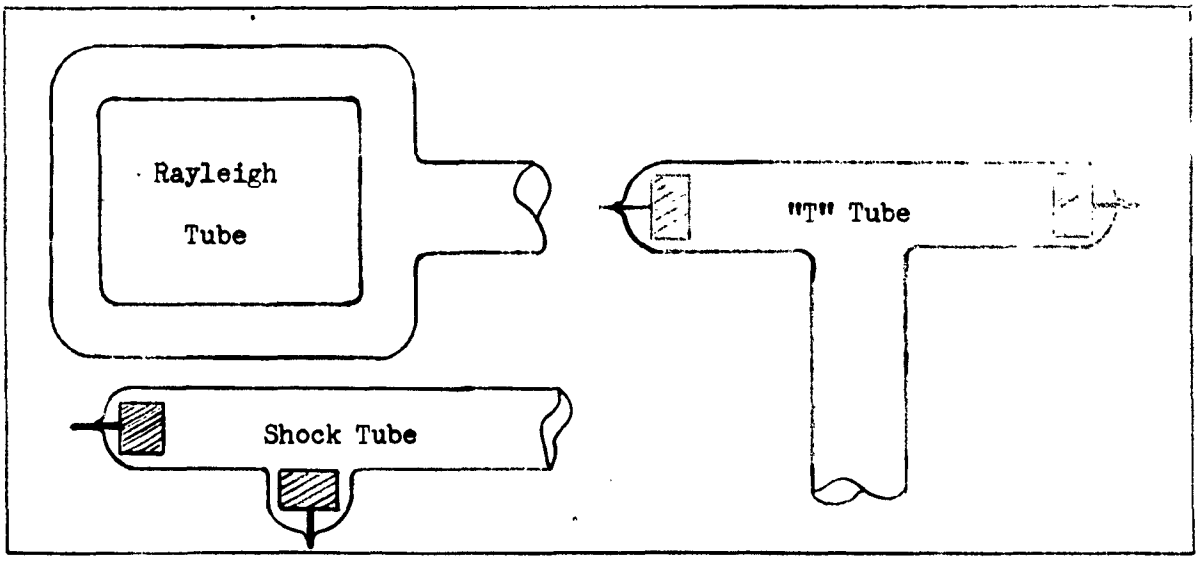


Fig. 3. Various tube styles used during the course of this research.

The size and composition of the discharge tube had rather large effects on the discharge which have not been investigated in sufficient detail to describe here. The discharge should yield much interesting information about the behavior of ionized gases at solid surfaces.

5. Spectrographic equipment.

Standard spectroscopic equipment was used in these investigations. A Hilger E-1 Littrow type quartz spectrograph (f:30) was employed for high resolution work, and a Leiss cornu prism spectrograph (f:16) was useful for survey purposes.

In some situations, such as the ion concentration studies, it was convenient to image the tube on the slit of the spectrograph, so that a point by point record of the tube's luminosity could be obtained. In others, like the radiation law studies, the tube was placed close to the slit of the spectrograph so that light from a limited area of the tube (about 1 $cm^2$) filled the collimater. Photometry of the spectral lines was carried out on a Knorr-Albers microphotometer.

Accurate plate calibration with a discharge of the brevity of this one posed a problem of some difficulty. Our solution was to compare a series of spectra taken with multiple discharges of the tube on the assumption that reciprocity law failure was small, and that any intermittency effect was eliminated by the intercomparison of the data. This assumption is countenanced in some degree by Mees and by information supplied by the Eastman Company on its materials. It was further borne out by the agreement between data taken at different levels of intensity.

6. Vacuum systems.

Conventional vacuum technique was employed. Stopcocks were lubricated with low vapor pressure greases such as Apiezon "M" and "N" greases and Dow-Corning high vacuum silicone grease. In all refined experiments liquid air

traps were used to isolate the discharge from the stopcocks. Despite these precautions, the discharge invariably showed the spectrum of carbon, as well as spectra of the wall and electrode materials.

A special dual range Macleod gauge was designed for this work. By using two measuring capillaries of different size stacked with the smaller on top, and making two fiducial marks, one at the top of the small capillary, and one at or near the top of the large capillary, it was possible to have a dual range gauge in which the ranges overlapped enough for precision measurement on all scales. A correction on the large capillary scale was needed for the unused volume above the lower fiducial mark. The gauge measures pressures from $10^{-5}$ to 20 mm Hg, and has the added advantage that it is often possible to detect the presence of condensible vapors by comparing the readings on the two scales.

Hydrogen gas was purified by being admitted through palladium, and all other gases except air were purchased as spectroscopically pure.

7. Special detectors.

The many phenomena present in the discharge have required a variety of detectors to gather the necessary information. In addition to the studies which have been conducted with the wave speed camera and spectrographs, we have studied the electrical characteristics of the discharge, the speeds of the invisible shocks, the pressures of shocks, and the ion concentrations and flow speeds. All these phenomena are necessarily of a transient nature, and have been studied by observing suitable electrical signals with a Tektronix 514D oscilloscope.

To measure input energy to the discharge we have used a resistive potential divider for voltage measurement and a calibrated resistance for current measurement. Considerable technical difficulties had to be overcome in both measurements to eliminate unwanted signals of inductive origin. In the current measurement this was accomplished by using a short section (.025$\Omega$) of 1/4"

graphite rod, with a close-fitting coaxial brass tube as a return circuit. The tube and rod were separated by a very thin layer of insulation. Inductive effects were negligible up to current fluctuations of $10^9$ amp./sec.

To measure shock speeds a number of devices were tested and abandoned in favor of a magnetic microphone. Glow discharges (15) were found to be sensitive to several characteristics of the discharge beside the pressure changes, and their patterns could not be interpreted adequately. Photoelectric cells responded too greatly to the light scattered from the glass of the tube. Piezo electric crystals were strongly disturbed by inductive effects. A magnetic microphone in which the diaphragm was made of .003" steel shim stock proved the most satisfactory. It responded to shocks well within one $\mu$sec. of their arrival. Although this pickup was so large that it could only be used as an obstacle to terminate the free travel of the shock and reflect it, it was decided to use it to obtain as much information as it would give.

8. Special electronic devices.

A difference amplifier has been designed and constructed which has proven to have excellent fidelity from $10^4$ to well above $10^6$ cps. The lower limit could easily be extended at will. The circuit is given in Fig. 4.

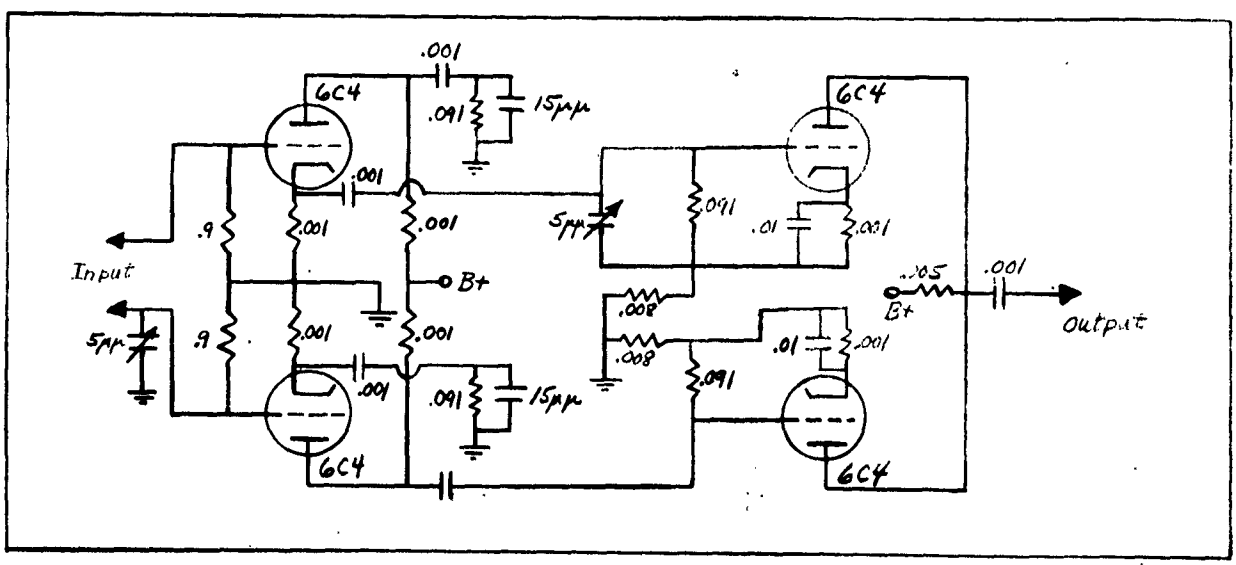


Fig. 4. Difference amplifier. Unlabeled capacitances in microfarads, resistances in megohms.

## CHAPTER III

## EXPERIMENTAL RESULTS

Wave speed camera studies.

The major effects observed in the wave speed camera pictures are summarized well by Fig. 5. The gas in the discharge chamber is rendered strongly luminous during the passage of the discharge current (the discharge is of the order of $10^7$ times as intense as a glow discharge). It then expands rapidly into the expansion chamber, expanding and remaining luminous even after the current has subsided. The expansion is preceded by a shock wave in the expansion chamber gas which may be self luminous. The shock reflects if obstacles are present in the expansion chamber, and when returning back up the expansion chamber eventually encounters the oncoming luminous gas which has been flowing out of the discharge chamber. The boundary between the strongly luminous expanding gas from the discharge tube and the less luminous gas which it is pushing away and which was originally in the expansion tube is properly called a contact-surface. The shock crosses the contact-surface, reverses the direction of flow of the outflowing discharge-chamber gas, and contirues onward through it. Both the shock and the luminous flow show marked decelerations and accelerations while expanding outward on several occasions during the expansion. In Fig. 5, these effects are all clearly visible. The upper end of the discharge chamber is all that was photographed. The discharge chamber lies wholly below the line CC'. It is brilliantly luminous during the discharge of the capacitor between times TT'. At E the expansion commences. At S the shock separates from the expanding gas. At D the shock and expansion show a marked deceleration. At P the shock reflects off the piston-like obstacle which can be seen in the photograph by its own scattered light. At I there is an interaction with the oncoming contact-surface. The direction of gas flow in

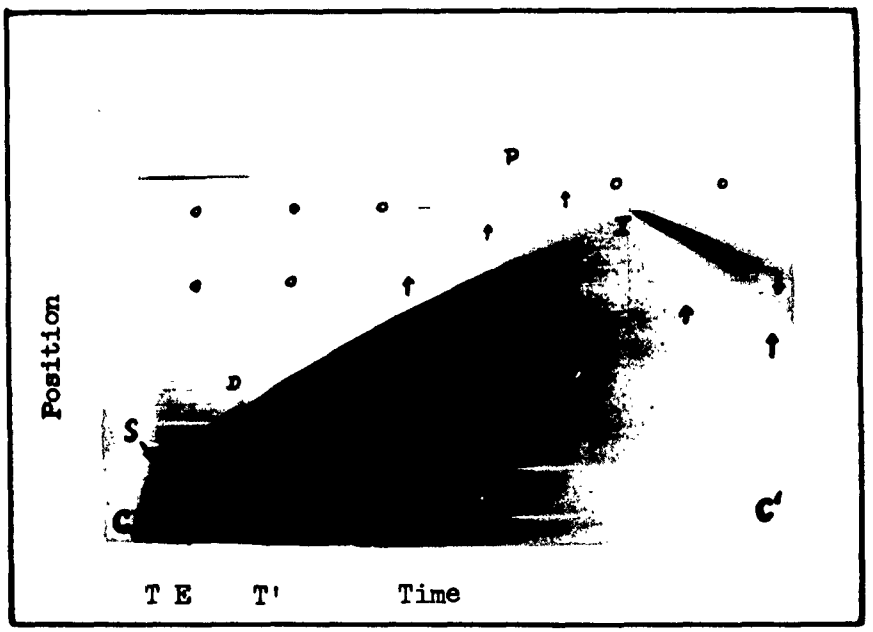


Figure 5. Wave speed camera photograph of gas expansion in argon discharge. Shock world line has been retouched for printing.

various regions is shown by arrows. Regions where gas is at rest are shown by zeros.

Analysis of the contact surface velocities for argon, helium, hydrogen, neon, air and nitrogen has shown that they are proportional with fair accuracy to the square root of the initial capacitor energy per unit mass of gas in the discharge. The relation has been tested in various discharge tubes with different discharge circuit constants, and is in general correct, although the slope of the curve is somewhat sensitive to the constants of each particular circuit. A typical set of data is plotted in Fig. 6.

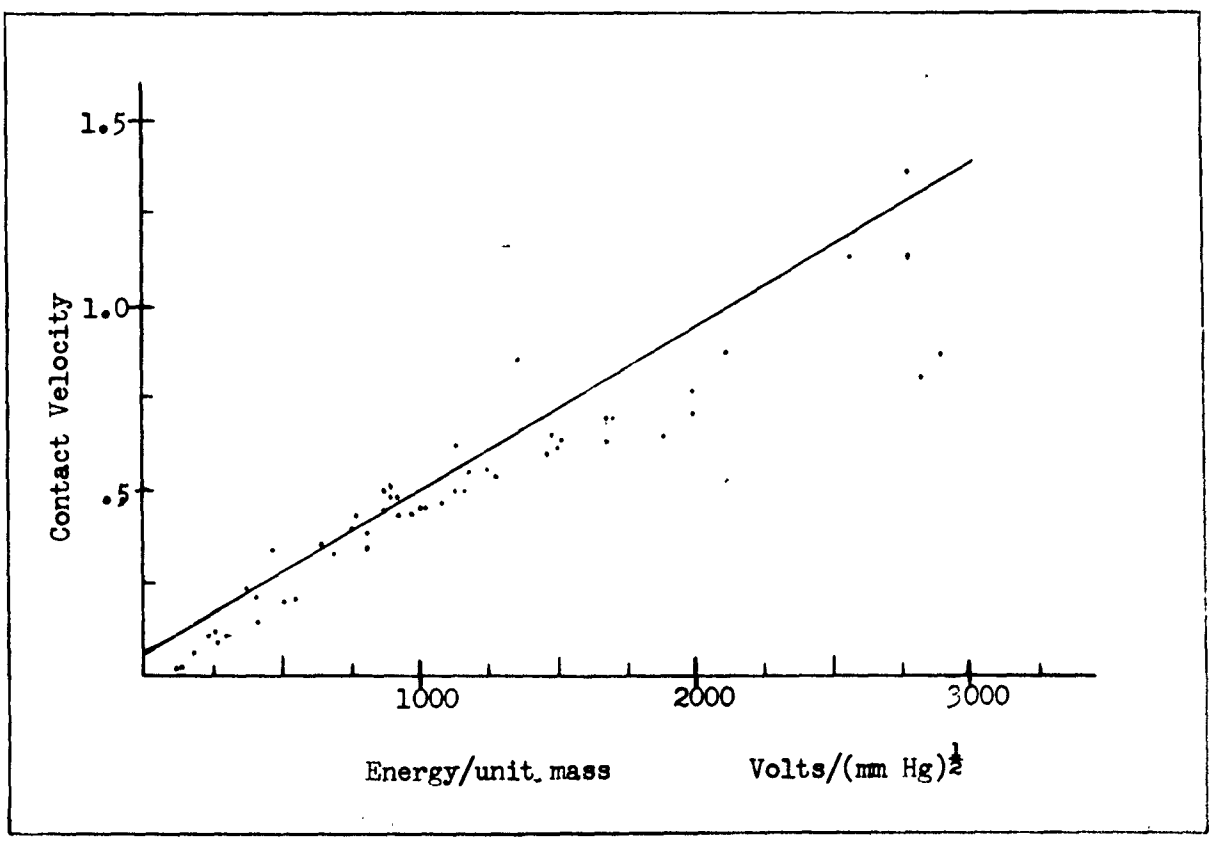


Fig. 6. Experimental relation between observed flow speeds and input energy.

Two independent measurements have confirmed the velocities measured with the wave speed camera as being true gas flow velocities. By discharging "T" tubes so that the fronts moved along the axis of the spectrograph in both direc-

tions, toward and from the slit, it was possible to observe Doppler shifts in the light emitted by the discharge. The Stark broadening of the hydrogen lines made them of little use in this experiment, although at extreme velocities even these lines showed a slight but perceptible shift. The effect was most pronounced in the impurity elements such as carbon which do not show first order Stark effect, but which were swept along by the current of hydrogen atoms. The observed shifts were in order of magnitude agreement with the mirror measurements on front velocities. A comparison of approximate measurements is given in Table 3.

Table 3
Doppler Effect

| Estimated Doppler Velocities | Comparable Mirror Velocities |
|---|---|
| 28.0 Km/sec | 18.0 Km/sec |
| 39.0 | 20.0 |

A second test of the gas flow velocities was made using the Hall effect. When the flowing ionized gas is made to pass between floating probes in a uniform magnetic field, a potential difference appears across the probes which is proportional to the flow velocity of the gas. Very good agreement has been shown between the data from this method and that from the wave speed camera. Comparative measurements are given in Table 4 taken in the same tube, at the same point along the flow at which the magnetic measurements were taken. However, the mirror used was inferior to our standard equipment, and the measurement of the contact speed is subject to considerable unknown inaccuracy. The Hall effect measurements are $\pm 10\%$ accurate on an average. In any case, the Doppler shifts and Hall effect both contribute evidence to support the view that the moving luminosity is a true gas flow.

The effects accompanying the reflection of the shock wave depicted in Fig. 5 were the first definite evidence which established the nature of the

Rayleigh phenomenon as a fluid flow. Analyzed in the language of fluid mechanics, the shock in the exterior gas moves through that gas until it meets the obstruction. Then the shock condition changes from a requirement that gas originally at rest be promptly and discontinuously accelerated, to one that gas then

Table 4

Hall Effect Measurements

| Hall Velocity | Mirror Velocity |
|---|---|
| 8.2 Km/sec | 8.1 Km/sec |
| 7.1 | 7.8 |
| 6.2 | 6.8 |
| 7.4 | 6.5 |
| 7.8 | 6.2 |

in motion come promptly and discontinuously to rest. Both conditions produce changes of entropy in the exterior gas. The reflected shock on its return trip eventually encounters the contact surface and undergoes an interactive acceleration in passing from one gas to the other. Thus the observed reflection of the contact surface before reaching the reflecting obstruction indicates that a compression of the exterior gas has occurred to such a degree that the expanding interior gas is brought to rest before reaching the obstruction. From this premature reflection of the contact surface the existence of a primary shock wave in the exterior gas was first inferred.

Subsequently, experiments were performed in which the primary shock and reflected shocks were both made visible in their own emitted light under properly chosen conditions of gas pressure, and input energy. Fig. 5 was taken under these conditions. While accurate studies of the onset of this self luminosity have not yet been made, a few general facts are known. The original gas density is the most important factor governing the onset. At some value of the

density characteristic of each kind of gas, a transition occurs from non-luminous shocks to luminous ones. As the density is further decreased the primary shock becomes progressively more luminous and the gas flowing behind the contact surface becomes less luminous until finally at extremely low pressures the shock front is the only luminous manifestation of the expansion. Under these latter conditions the luminosity travels up to intimate contact with obstructions in the tube instead of reflecting before reaching it as is typical of contact surfaces. The reflection is therefore a good test for the nature of the front under observation. The approximate densities for onset of the transition are given in Table 5.

Table 5

| Gas | Approximate Pressure of Transition |
|---|---|
| $H_2$ | 7 mm |
| He | 4 mm |
| A | 1 mm |

This result explains the anomalies which are present in our earlier reports (8,9) where we have described the expanding post-discharge luminosity of the spark as being in some cases a ball of flame and in others more nearly a luminous tongue or jet. The shock is ball-like in intensity distribution, while the contact surface luminosity is tongue-like. We believe that this transition in the post-discharge disposal mechanism of surplus excitation energy may well be a critical point for the definition of the term <u>low pressure spark discharge</u>.

A crucial experiment was performed as a direct test of the expansion hypothesis. The discharge chamber was separated from the expansion chamber initially by a parlodion film 1000 A° thick. Different gases were placed on opposite sides of the film. In one case hydrogen was used as the interior gas,

with (1) helium, (2) vacuum, and (3) a helium and hydrogen mixture all being tried as the exterior gas. In a second case helium was used as the interior gas, with (1) argon, (2) vacuum, and (3) an argon and helium mixture as the exterior gas. The entire discharge tube, main chamber and expansion chamber, was then imaged on the slit of the Leiss spectrograph. The results were the same in any case. No luminosity characteristic of the exterior gas was observed. The luminosity from the interior gas was present at large distances (20 cm) down the expansion tube. The spectrum of the parlodion film was strongly excited, and the spectrum of the electrode material was clearly in evidence.

It is certain from this experiment that the interior gas actually expands. It is probable that the luminosity induced in the exterior gas in these experiments was of a lower order of intensity than that in the interior gas, and hence did not record. The presence of the volatilized parlodion film may have acted as a buffer between interior and exterior gas also. The experiment is being repeated with greatly increased precautions against hydrocarbon impurities to simplify the interpretation.

The entire flow process promises to be an interesting tool for the study of unusual fluid flow situations. Interactions in one-dimensional flow have been observed which cannot be observed easily with conventional shock tubes. Shocks have been made to overtake or collide head on with contact surfaces. As yet, however, no certain evidence has been obtained of the existence of a rarefaction wave in the ionized interior gas. There is no indication that it overtakes the shock, as it should, nor is there any regular appearance of a progressive intensity reduction in time and position in the light from the region between the electrodes, although anomalous behavior which might be related to a rarefaction has been observed in a few cases. Three such cases were depicted in Fig. 21 of our December 31, 1951 report on this project (14).

Electrical characteristics.

Edgerton and Murphy (15), and Olsen and Huxford (16) have reported briefly on measurements of the electrical characteristics of flash tubes somewhat similar to ours. Two essential differences exist between their tubes and ours. The pressures are much lower in our tubes, and the gas is permitted to expand during the discharge. We have therefore carried out a detailed study of the currents in and potentials across the discharge tube under a variety of conditions. The results will only be reported in part here, because the final purpose is to use them in conjunction with shock and flow speed studies. Curves of instantaneous potential, current, power and resistance are given in Figs. 7, 8, 9, and 10 for a variety of conditions.

Mechanisms of the luminosity.

Extensive spectroscopic studies of the discharge and the expansion have been made, to cast light on the mechanisms which are responsible for the production of radiation in the discharge and afterwards. The Stark broadening of the Balmer series in hydrogen has been investigated in detail in T-shaped tubes and shock-type tubes. There is no essential difference between the broadenings characterizing expanding interior gas when it is ejected from either the T-tube or from the shock tube. There is also no noticeable dependence upon discharge polarity in the broadenings observed during the expansion in a shock-type tube.

Half-widths of the broadened Balmer lines $H_\alpha$, $H_\beta$, $H_\gamma$, and $H_\delta$ were measured as a function of position along the expansion tube for several gas pressures and several capacitor potentials. Each value is the average of three to five measurements at as many levels of exposure. The over-all agreement between half-widths measured at different exposures was quite good, the deviation from the mean being 13 percent.

The half-widths $\delta$ were interpreted as a measure of ion concentration according to the relation of Holtsmark

$$\delta = 3.25\ A e n^{2/3}.$$

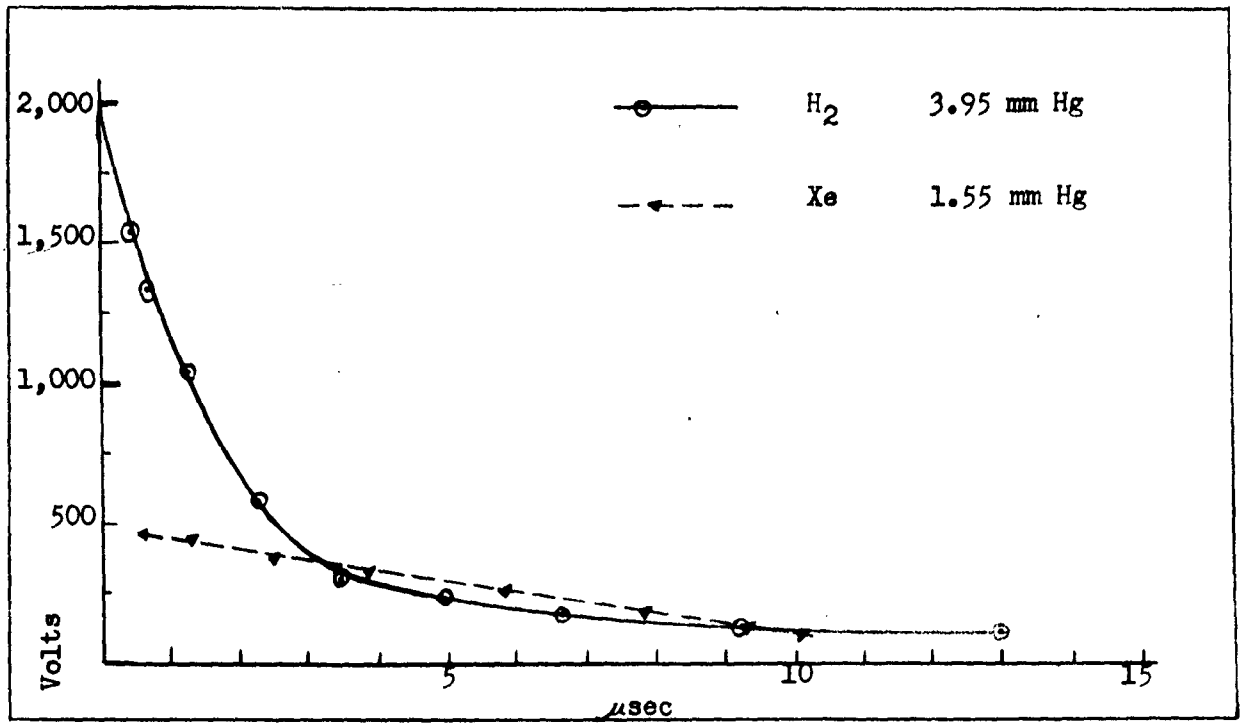


Fig. 7. Time variation of tube potential.

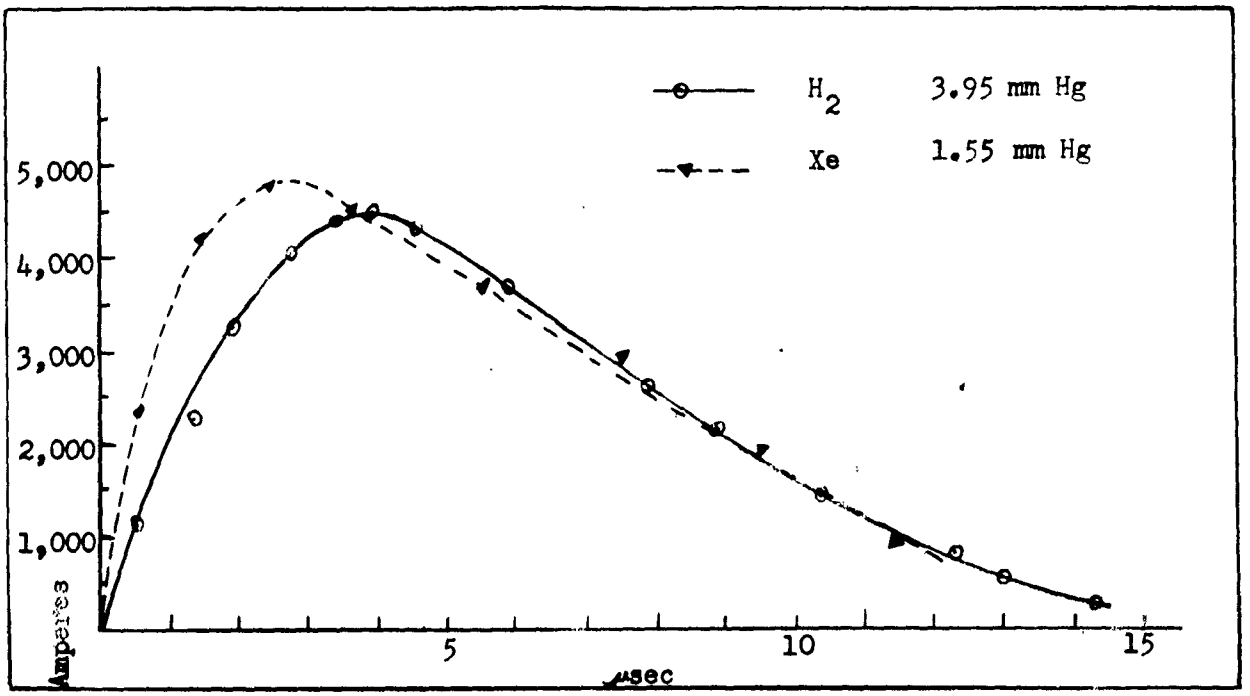


Fig. 8. Time variation of tube current.

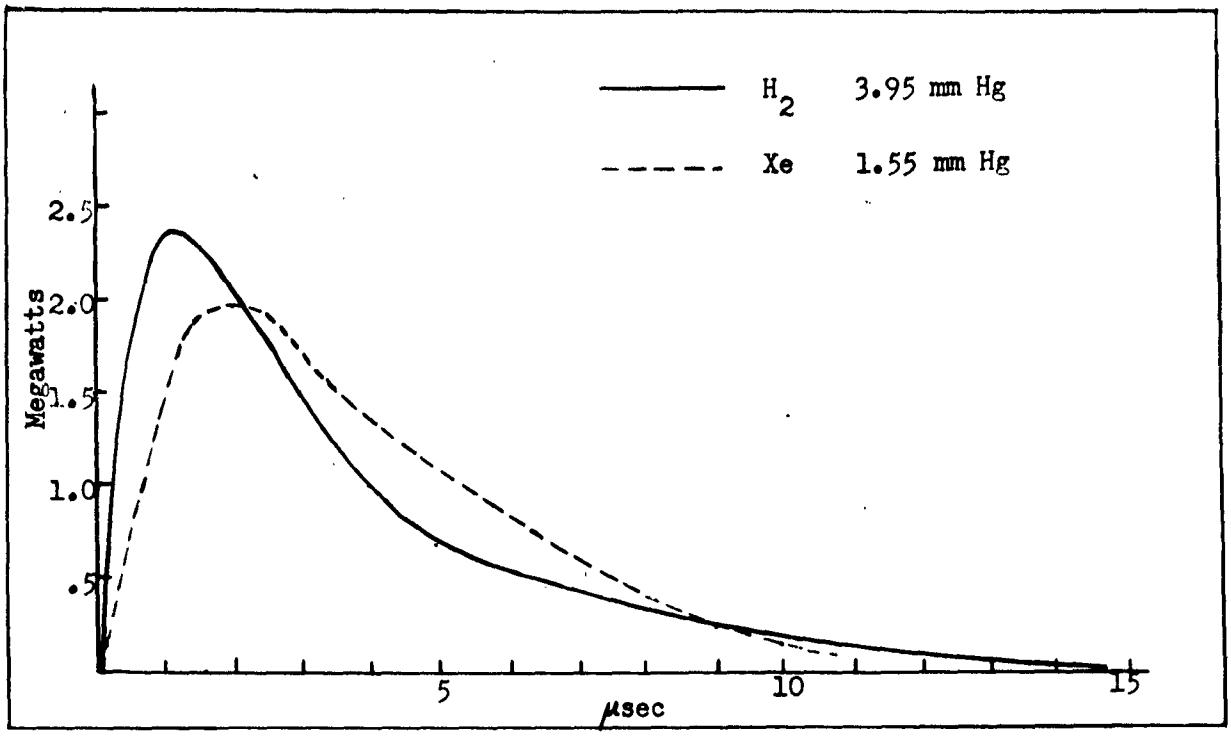


Fig. 9. Time variation of power input.

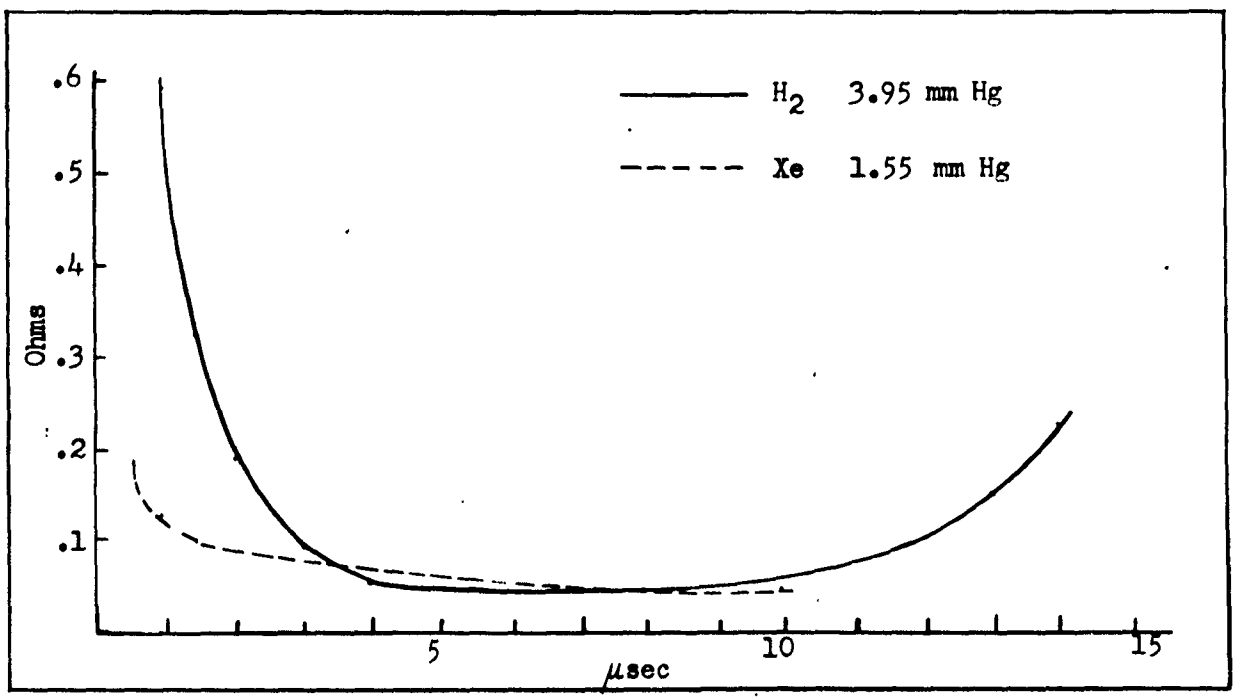


Fig. 10. Time variation of tube resistance.

Data computed in this fashion are given in Figs. 11 and 12. These data are weighted averages of the results from all four of the Balmer lines. In the application of Holtsmark's theory, estimation of the Stark coefficient A is a critical matter. Holtsmark defined it as the separation in $cm^{-1}$ per unit field between the extreme Stark components of the line in question. He further assumed a uniform distribution of energy between the outermost components. As he was aware, and as Fig. 13 shows, this is not the case in actuality. Ion concentrations calculated on these assumptions do not show very close agreement between the results reported by different lines of the Balmer series. Considerable improvement can be made by replacing the separation between extreme Stark components by the separation between the widest pair which is strong enough to contribute significantly to the line intensity. In some cases, the extreme component is so weak that it has never as yet been detected experimentally.

While this change brings the two Holtsmark assumptions into better accord, there is still one feature of the component array which is completely neglected by the Holtsmark theory. The odd members of the Balmer series have a strong undeviated component which the even members lack. This results in a sharp peaking of the $H_\alpha$ and $H_\gamma$ lines in comparison to the $H_\beta$ and $H_\delta$ lines. A microphotometer tracing which shows this effect is given in Fig. 14. This characteristic serves as an identifying criterion for Stark broadening, but makes the calculations of ion concentration from the odd series members too low.

We have observed another effect which we believe also originates in the Stark effect, which will tend, on the other hand, to make the results from the even members too high. In the presence of extremely high fields, the $H_\beta$ line is observed to be doubled. This is not ordinary self reversal because it is not shown by the other members of the series. It seems probable that it comes about because of the great vacancy in the center of the array of the even

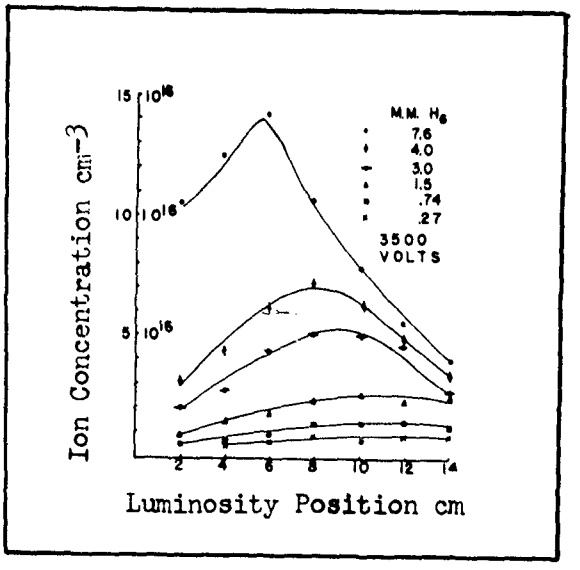


Fig. 11. Ion concentrations at constant voltage.

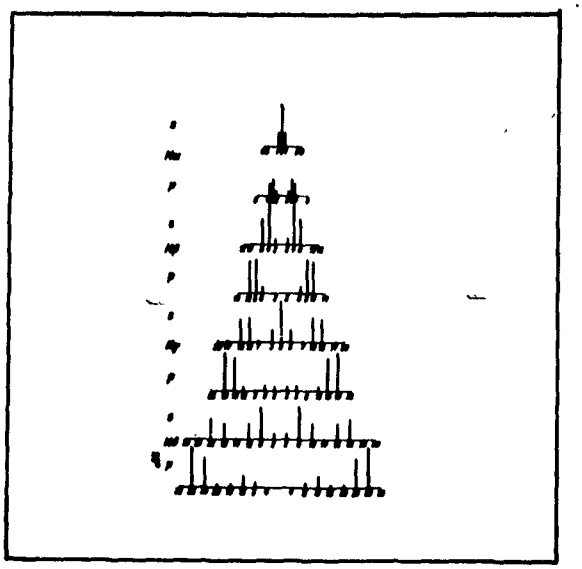

Fig. 13. Stark components of the Balmer lines.

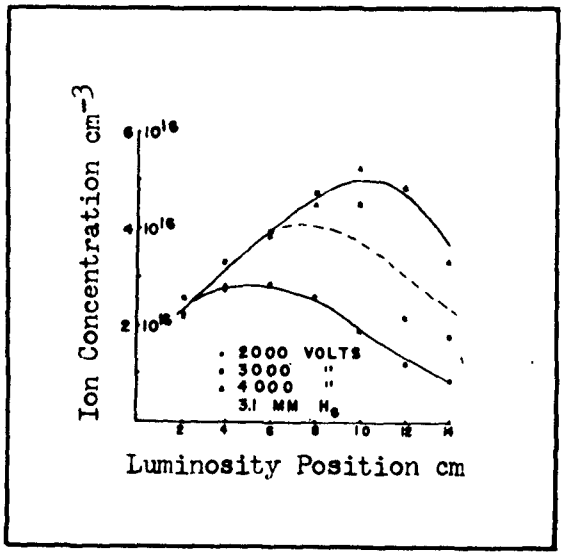


Fig. 12. Ion concentrations at constant pressure.

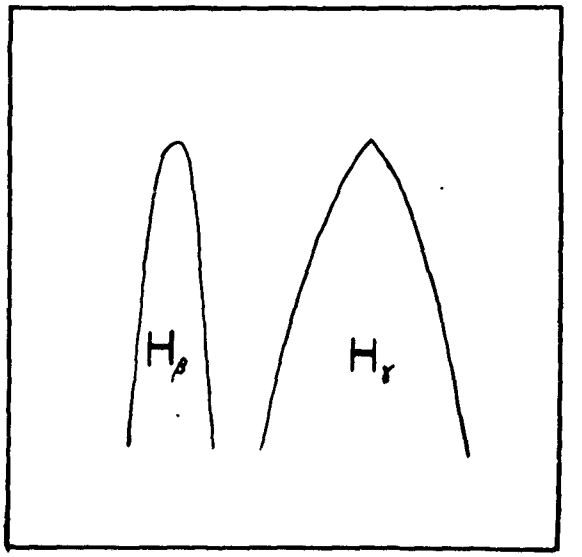


Fig. 14. Contours of $H_\beta$ and $H_\gamma$.

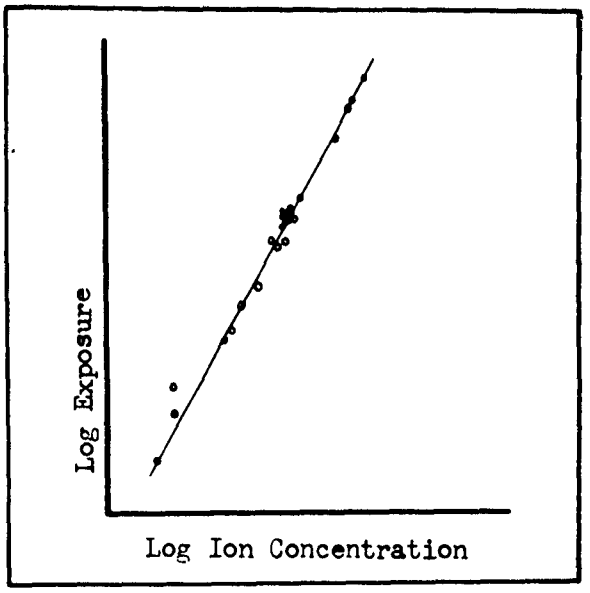


Fig. 15. Exposure versus ion concentration.

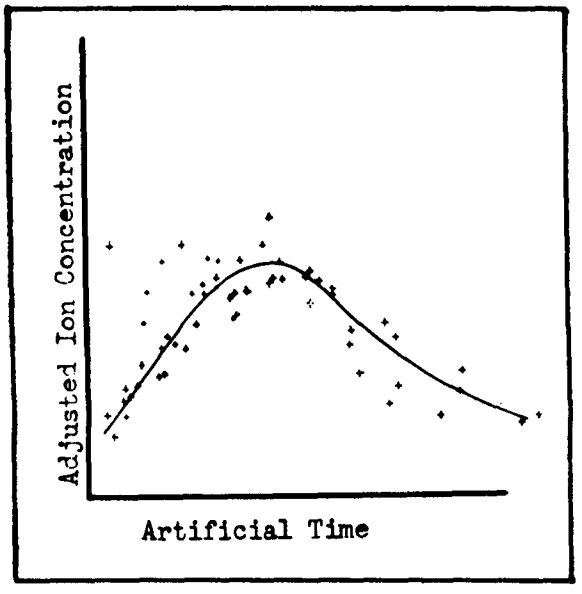


Fig. 16. Ion concentration versus artificial time.

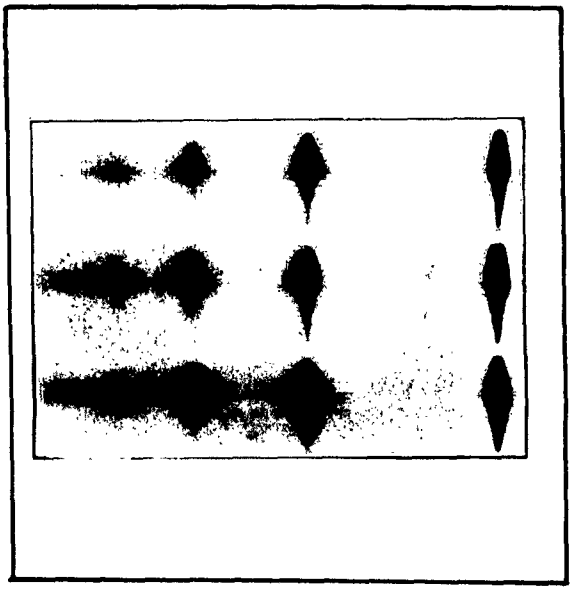

Fig. 17. Stigmatic spectrum of $H_2$ covering 14 cm of the expansion chamber.

components. Holtsmark's distribution function for random fields has a maximum probability at a finite value of field intensity, and a zero probability of zero field. These two causes may combine to produce the splitting of $H_\beta$ in strong random fields. The Holtsmark relation suggests another simple test for Stark broadening. The ratios of the half-widths of the various Balmer series members under any given condition are independent of ion concentration and strictly porportional to the ratios of the separations of the outer Stark components selected as discussed above. These ratios are given in Table 6. The agreement is best between lines of similar contour. The material of which the tube wall is composed has a considerable effect on the ion concentration observed. Higher concentrations are present in quartz tubes than in pyrex. This fact is inferred from the extinction of the Balmer series at lower values of n in the latter case, although no measurements have been made as yet on line broadening. In pyrex, the Balmer series terminates at $H_\theta$, in quartz at $H_\epsilon$. Von Traubenberg (11) has shown that the complete washing out of the upper quantized states of an atom is a measure of the Stark fields in which the atom is placed. This approach can be used to obtain an independent estimate of the ion concentration, but has been neglected here in favor of the line broadening technique.

A special treatment of the ion concentration data reveals a regularity in the discharge which has not yet been explained. If the abscissas (positions along the expansion chamber) are divided by the initial velocity of the fronts to obtain a time, which we call a "synthetic" time, and the ordinates are divided by the product of gas pressure and capacitor potential, the data at all capacitances and gas pressures can be represented on a single graph within the experimental error. This graph is given in Fig. 16.

The total energy radiated in the broadened line can be measured by integrating intensity over wave length. At two selected positions along the

discharge tube, total integrated exposures and half-widths were measured simultaneously using the $H_\beta$ line. Two methods of obtaining the integrated exposures were used with equal success. First, after study of several representative line contours had shown them to be of nearly Gaussian profile, the product of the maximum exposure and half-width for each line was used as a measure of the integrated exposure. Second, several actual profiles were converted from blackening to exposure, point by point, and planimetered as a check on the first method. This second method would be the method of choice were it not for the enormous amount of computation needed.

Table 6

Internal consistency of half-widths

| Lines | Experimental average ratios | Theoretical ratios |
|---|---|---|
| $H_\gamma/H_\beta$ | 1.3 | 1.8 |
| $H_\delta/H_\beta$ | 2.7 | 2.8 |
| $H_\delta/H_\gamma$ | 2.2 | 1.6 |

An investigation was next made of the relation between ion concentration as determined above, and the total integrated intensity of the $H_\beta$ line. A logarithmic plot of these intensities against half-widths interpreted as concentrations is given in Fig. 15.

In actual fact, the quantity measured was not intensity, but exposure. Since the fronts at various pressures (and hence at different ion concentrations) pass the spectrograph's field of view in different time intervals because of their differing speeds, one might expect that a velocity correction should be made on these exposures to give a quantity more nearly proportional to the intensity. To make this correction the exposures should all be multiplied by

the velocities of advance of the luminosities. No correction has been made on the data of Fig. 16. To make corrections results in a much greater scatter of the experimental points, and introduces systematic differences between the points obtained with different capacitors. Since the uncorrected data are always superior in agreement to the corrected data, it seems probable that these corrections should not be made. Analysis of the problem has shown, however, that it is not possible to decide whether the correction should be made on a basis of simple arguments like those above. Uncorrected, the slope of the integrated exposure-ion concentration curve is 1.9, a value which we interpret as 2, within the experimental error. A quadratic dependence of intensity upon ionconcentration would be conclusive evidence that the production of quantized radiation comes almost entirely through the intermediary step of recombination. It does not follow inexorably that because the integrated exposure varies as the square of the ion concentration the integrated intensity must also exhibit this dependence, but it is plausible, and the time resolved intensity studies of Olsen and Huxford strongly suggest that this relation would have been found if we had measured intensities rather than exposures.

A further investigation of ion concentrations and integrated intensities was made in the shock-type tube, confirming in every respect the results of the T-tube at all points in the expansion chamber, but adding new information about the post-discharge behavior in the region between the electrodes. The Stark broadenings indicate that there is always a minimum of ion concentration lying opposite the electrode which separates the main discharge chamber from the expansion chamber. Whereas the position of the ion concentration maximum which is observed in the expansion chamber is very sensitive to input energy, the position of the minimum was invariable under the range of conditions of this experiment, and probably is truly fixed in position for all conditions.

Two other facts were observed in the shock tube. When the direction

of charge flow is reversed the distribution of ion concentrations and intensities is unchanged. We deduce from this that the entire luminosity mechanism is independent of the charge conduction processes. This is in full accord with the belated emission of the radiation. Second, the intensity and broadening in the discharge increases point by point as we move from the chamber-separating electrode up the main chamber to the end electrode. At this point the broadening of $H_\beta$ is as great as at any place in the expansion chamber, but the intensity of $H_\beta$ in the discharge is far less than at the exterior maximum. Furthermore, the square law intensity relation which holds throughout the expansion chamber fails completely in this region between the electrodes. It must be emphasized that these observations apply to the $H_\beta$ line, and hence to the quantized radiation only. The continuous radiation, which accounts for a large proportion of the luminosity, very probably obeys different laws as the work of Olsen and Huxford shows.

The intense continuum associated with the Balmer series deserves careful study. A spectrum of the discharge is given in Fig. 17. The origin of this continuum had not been definitely established at the time this project began (the recent work of Olsen and Huxford had done much to clear up the question). Some authors have assigned it a molecular origin, while others speak of it as a "pressure" continuum, although the implication that it is caused by pressure processes seems doubtful. Experiments were therefore conducted to establish additional facts about it.

An attempt was made to detect the existence of a similar continuum in the vicinity of the Paschen series. Inferior dispersion and the rapid fluctuation of sensitivity with wavelength for Eastman Z plates made it difficult to interpret the spectra obtained, but a continuum was definitely observed. Whether the distribution of intensities in this continuum was similar to that of the Balmer associated continuum is debatable. The impression given by subjective

study of the plates and photometer tracings is that the Balmer associated continuum is considerably more far-flung than the Paschen continuum, extending as it does from some point between the series members at around 5000 A to a point well below 2000 A.

To investigate the possible molecular origin of the continuum, water vapor was substituted for hydrogen gas in the discharge. Before each discharge the tube was carefully pumped out to remove any hydrogen which might have formed by dissociation during the previous discharge. The spectrum of the Balmer associated continuum was identical in every detail with that obtained in pure hydrogen. A few additional lines caused by the oxygen atoms were present in the spectrum. The continuum cannot, therefore, be caused by molecular dissociation in $H_2$.

Contrast of the Balmer associated continuum with the molecular continuum obtained from a glow discharge shows a considerable difference in the distribution of intensities, and calls attention to two other features of distinction: the thousandfold disparity between the intensities of the two continua, and the multiline spectrum which accompanies the molecular continuum but not the Balmer associated continuum.

It seems certain that at least part of the Balmer associated continuum is caused by recombination processes. Unless, however, the random fields of the ions produce some sort of enhancement and Stark broadening of the continuous levels of the atom as well as of the discrete levels, it seems probable that another process than recombination is responsible for a large part of the continuum. Another fact which points to this conclusion is that continua are observed in about this same general region 5000-3000A with all of the other gases which have been used, argon, neon, helium, and nitrogen. Hahn and Finkelnburg, and Olsen and Huxford have suggested that a bremsstrahlung process may be needed to explain this.

Spectrograms of the discharge in $H_2$ at pressures less than 1 mm show the tube wall is decomposed during the discharge. The spectra of these wall impurities have shown that excited systems having energies 167 ev above the ground state are present 5 cm down the expansion chamber. Silicon IV lines were graded in intensity, the lines being most intense at the head of the expansion chamber and becoming unobservable 5 cm down the expansion chamber. Silicon III lines had a slight intensity gradation and were visible 8 cm down the expansion chamber. Silicon II lines were visible throughout the entire 14-cm region investigated and had a maximum intensity 6 cm down the side tube. The lines of Silicon I were not present at all near the head of the expansion chamber, but were found throughout the lower 9 cm of the 14-cm region investigated. The ionized forms of oxygen showed analogous behavior.

Two alternative implications of the observed intensity distribution may be obtained. Assuming that the atoms are ionized and excited at the position where their spectra are observed, one would conclude that the energy available for ionization decreased with distance down the expansion chamber. On the other hand, assuming that the atoms are all ionized in the main discharge tube and that they then travel to the point where their spectra are observed, one would conclude that a Si atom starts its journey as Si IV and captures electrons as it moves down the tube, becoming successively Si III, Si II, and finally Si I. The latter theory is incompatible with the behavior of the ion concentrations. All indications point to this trend of the silicon excitations as an expression of the thermal equilibrium of the hot expanding gas, in which ionization is maintained by the electron cloud at a level compatible with the temperature. Each successive upper level is abandoned as the gas cools, with a corresponding increase in population of the lower levels. The increase results in an increased intensity of emission of the lines of these lower states. A further factor--that the recombination cross section decreases with electron temperature--

reduces the intensity of lower level transitions in the hot gas. High level transitions are made possible in spite of the high electron temperature because the recombination cross section is proportional to the ionic charge. It is our belief that the luminosity observed in the discharge is largely derived from the impacts of electrons in a hot gas in thermal equilibrium, via the agency of recombining ions.

This thermal equilibrium theory is countenanced by the Milne-Fowler color-temperature theories used in astrophysics. Table 7 gives the temperatures at which various levels of excitation, in thermal equilibrium, would reach their maximum radiated intensity. Data for this table is taken from the Handbuch der Astrophysik.

Table 7

| | | | |
|---|---|---|---|
| SiI | 7000° | H | 10,000° |
| SiII | 10,000° | CII | 16,500° |
| SiIII | 17,500° | OII | 17,500 |
| SiIV | 25,000° | CIII | 25,000 |
| HeI | 16,500° | OIII | 26,000 |
| HeII | 35,000° | CIV | 40,000 |

The location at which the maximum of each of these stages of excitation is observed can now be used as a rough index of temperature in the discharge. A table (Table 8) based on this sort of estimate is given below.

Table 8

Discharge temperature distribution in $H_2$ at 3500 V, .3 mm, T-tube

| Distance from head of tube | Temperature | Gas |
|---|---|---|
| -1 cm | 26,000 | OIII |
| -1 cm | 25,000 | SiIV |

Table 8 (continued)

Discharge temperature distribution in $H_2$ at 3500 V, .3 mm, T-tube.

| Distance from head of tube | Temperature | Gas |
|---|---|---|
| 1-2 cm | 17,500 | SiIII |
| 3-4 cm | 17,500 | OII |
| 5 cm | 10,500 | SiII |
| 9-10 cm | 10,000 | H |
| 12 cm | 7,000 | SiI |

Discharge temperature distribution in $H_2$ at 4500 V, 3 mm, shock tube.

| | | |
|---|---|---|
| -8 | 10,000 | H |
| -7 | 10,500 | SiI |
| 0 | 26,000 | OIII |
| 6 | 10,000 | H |
| 15 | 7,000 | SiI |

Recognition of the shock waves.

The existence of the shock, which was inferred from Fig. 5, has been confirmed by direct measurement of the time required before a microphone with a light steel diaphragm is disturbed by the shock. When the diaphragm is placed squarely across the tube so that it terminates the tube like one of the pistons described in the reflected luminosity experiments, it is possible to measure the time of flight of the shock from the moment of initiation to collision with the diaphragm. A plot of such a curve is given in Fig. 18, showing how an acoustically measurable shock rides in front of the contact as measured by the wave speed camera, even in a non-luminous case. There is also very good agreement between the acoustical measurements and wave speed camera measurements in the case of luminous shocks.

Peculiar phenomena.

There is considerable evidence that vacuum ultraviolet radiation is very intense in the exterior gas before the coming of the shock. Metallic objects present in the exterior gas acquire potentials of several volts, and considerable photoelectric currents can be drawn between electrodes. Further, discrepancies exist in the calculations of shock speed which could be reconciled by assuming a radiation preheating of the exterior gas. In no case, however, have we found that radiation enters into the production or propagation of luminosity to any major degree. Nevertheless, the trapping of radiation (resonance radiation in particular) may serve as a means of reducing the rate of emission from the gas, and hence of reducing the apparent value of the recombination coefficient. Olsen and Huxford have indeed observed what seemed to be abnormally low values of this coefficient under conditions similar to ours.

Photographically, using the wave speed camera, we have observed two examples of a phenomenon which fits the description of the spinning detonations well known to explosion chemistry. When the slit of the camera is transverse to the main discharge tube, a zigzag pattern is observed as if a luminous filament of smaller diameter than the inside diameter of the tube oscillated back and forth across the slit. When the slit of the camera is parallel to the tube, there is a slight periodic fluctuation of the apparent speed at which the contact surface moves. In yet another situation, rather large periodic fluctuations of the current to the probes are observed in the Hall effect experiments. These are believed to be caused by filamentary localizations of the ion cloud, and the periodicity of the fluctuation indicates strongly that it is caused by this same spiralling sort of flow pattern. No further investigation of the phenomenon has been made.

The expanding gas has a luminosity structure in time and space which has been the principal object of the research. We have successfully explained the

nature of the luminous flow and the existence of two fronts on the leading edge of the expansion as major phenomena. We have dismissed as trivial a number of irregularities such as second expansions produced by capacitor oscillations, and localizations of luminosity caused by inequalities in the inner surface and diameter of the tubes. After these have been set aside there remains a fluctuation phenomenon which seems to be well substantiated, and which we do not as yet understand. It occurs primarily in the main discharge tube, and is apparent as a repeated rekindling of the discharge after nearly complete extinction. Nearly all the mirrorgrams show it to some extent and since we have taken tube current and tube potential records simultaneously, we can say with some assurance that there were no corresponding fluctuations of discharge current or potential.

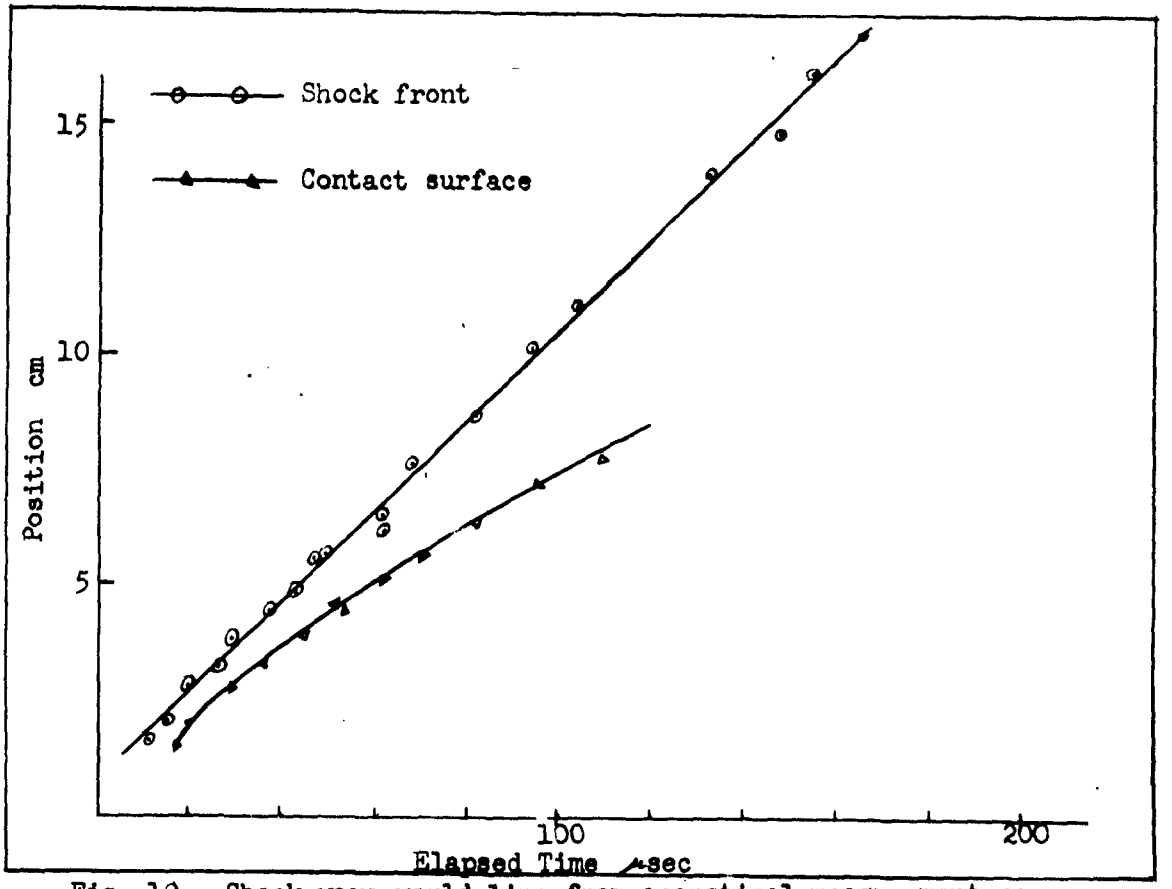


Fig. 18. Shock wave world line from acoustical measurement, compared with contact world line from wave speed camera measurement.

## CHAPTER IV

## THEORETICAL CRITIQUE

The mechanical aspects of the project have developed into a study of the validity of the equations of fluid dynamics under the extreme conditions present in low pressure gas discharges. The agreement obtained between theory and experiment is already adequate to establish the correctness of our theory of the expansion. In circumstances in which the shock and contact surface velocities could be measured simultaneously, calculations of the shock velocity which would be expected for a given contact velocity can be made from the equations of fluid flow. The particular relation used is given by Courant and Friedrichs (17). The interior gas is regarded as a piston following a prescribed motion, and the velocity of the shock is calculated from the equation

$$U_s = U_c/2(1-\mu^2) + \left[C_o^2 \quad \left(U_c/2(1-\mu^2)\right)^2\right]^{\frac{1}{2}} .$$

The results are in very good general agreement, considering the crude measurements which have been available until now. Table 10 gives measured shock speeds as $U_s^1$ calculated ones as $U_s$ .

Table 10

Comparative thermodynamic data for spark expansions. W = capacitor energy; $p_o$ = initial pressure; $U_c$ = contact velocity (luminosity); $U_s$ = calculated shock velocity; $U_s^1$ = measured shock velocity; $p_1$ = shock pressure; $T_1$ = shock temperature: $p_2$ = reflected shock pressure; $T_2$ = reflected shock temperature. Units used are joules, mm Hg, km/sec, 1000°K.

| W | $p_o$ | $U_c$ | $U_s$ | $U_s^1$ | $p_1$ | $T_1$ | $p_2$ | $T_2$ |
|---|---|---|---|---|---|---|---|---|
| 30 | 10 | 1.6 | 2.2 | 2.0 | 560 | 4.5 | 2100 | 10 |
| 120 | 0.8 | 4.0 | 5.4 | 5.1 | 280 | 27 | 1600 | 64 |

Table 10 (continued)

| W | $p_o$ | $U_c$ | $U_s$ | $U_s^1$ | $p_1$ | $T_1$ | $p_2$ | $T_2$ |
|---|---|---|---|---|---|---|---|---|
| 10 | 17 | 1.0 | 1.4 | ... | 380 | 1.9 | 1900 | 4.2 |
| 120 | 17 | 2.1 | 2.8 | 2.9 | ... | ... | ... | ... |
| 120 | 2 | 2.5 | 3.4 | 4.0 | ... | ... | ... | ... |
| 120 | 0.3 | 2.65 | 3.5 | 3.5 | ... | ... | ... | ... |
| 120 | 3.4 | 1.35 | 1.6 | 2.7 | ... | ... | ... | ... |
| 120 | 1.1 | 2.60 | 2.9 | 3.6 | ... | ... | ... | ... |

Using the assumption that the gas through which the shock advances is an ideal gas, computations of temperature and pressure are possible. These computations have been made for a few cases of the oncoming shock, and for the shock reflected from a plane obstacle. These latter figures give some idea of the origin for the observed luminosity. It is probable that we have to deal here almost exclusively with Saha temperature excitation processes. There is little doubt that fluid expansion theories of the post discharge luminosity are a proper basis for the bulk of observed phenomena.

It is possible to obtain a theory of the expanding interior gas which fits the data of Fig. 6 reasonably well. The theory of shock tubes in which the compression chamber is filled with a highly ionized gas does not differ from conventional shock tube theory if electromagnetic processes are not active in transferring energy from one portion of the flow to another. However, since the equations of state for a partially ionized medium are not simple, one must be satisfied with numerically obtained approximated solutions to the problems which arise. We will discuss the problem of finding the flow velocity. For simplicity's sake the experimentally well-justified approximation of instantaneous energy delivery by the capacitor will be made. The problem

then becomes that of finding u, the expansion velocity for given values of $e_2$, $\tau_2 = \tau_o$, and $p_o$.

$e_2$ = internal energy per gram of gas in the compression chamber immediately after the capacitor discharges.

$\tau_2$ = specific volume of gas in compression chamber immediately after the capacitor discharges.

$\tau_o$ = specific volume of gas in expansion chamber immediately after the capacitor discharges.

$p_o$ = pressure in shock tube before the capacitor discharges.

The thermodynamic behavior of the medium is approximated by the equations below which neglect excited states and multiply ionized atoms. The gas is here assumed to be monatomic.

$$S = \frac{5}{2}k\,\frac{1+\alpha}{m} + \frac{k}{m}\ln\left(g_a^{1-\alpha}\, g_I^{\alpha}\, g_e^{\alpha}\right) + \frac{I\alpha}{T} + \frac{k(1+\alpha)}{m}\ln\left[\frac{\tau m(2\pi kT)^{3/2}}{h^3}\right]$$

$$+\frac{k}{m}\ln m^{3/2} + \frac{k(1-\alpha)}{m}\ln\frac{1}{1-\alpha} + \frac{k\alpha}{m}\ln m_e - \frac{2k\alpha}{m}\ln\alpha .$$

$$e = 3/2\, p\tau + I\alpha .$$

$$p\tau = \frac{(1+\alpha)kT}{m} .$$

$$\ln\frac{\alpha^2}{1-\alpha^2}p = -\frac{mI}{kT} + \frac{5}{2}\ln T + \text{Const.}, \text{ (Saha's equation).}$$

S = entropy per gm,

k = Boltzman constant,

$\alpha$ = fraction of atoms which are ionized ($0 \leq \alpha \leq 1$),

m = mass of atom = mass of ion,

$g_a$ = statistical weight of atom,

$g_I$ = statistical weight of ion,

$g_e$ = statistical weight of electron = 2,

I = energy of ionization in ergs/gm,

T = absolute temperature,

$\tau$ = specific volume,

$h$ = Planks constant,

$m_e$ = mass of electron,

$e$ = internal energy (ergs/gm),

$\varphi$ = pressure,

$c$ = constant of medium = $\ln \left[ \frac{g_I g_e}{g_a} \frac{(2\pi m_e)^{3/2} k^{5/2}}{h^3} \right]$ .

From the four given equations one can find the four unknowns $\varphi_2$, $\alpha_2$, $T_2$, and $S_2$ corresponding to conditions in the compression chamber immediately after the condenser has delivered the specified energy $e_2$. As a result of the pressure difference $\varphi_2 > \varphi_o$, a shock wave moves through the gas in the expansion chamber raising the pressure from $\varphi_o$ to $\varphi_{1s}$ and imparting a velocity $u_{1s}$. Simultaneously a rarefaction wave moves through the gas in the compression chamber and reduces the pressure from $\varphi_2$ to $\varphi_{1r}$ and gives it the velocity $u_{1r}$. From the differential equations governing fluid flow one obtains

$$u_{1R} = \int_{\varphi_2}^{\varphi_{1R}} \frac{\tau(\varphi)\, d\varphi}{c(\varphi)} .$$

The entropy is kept constant in performing the integral since the expansion does not change from its initial value $S_2$. The expansion will change $\tau$ and also c, the sound velocity, however, since $S_2$ is not changed, both $\tau$ and c may be considered functions of $\varphi$ alone for a given energy input $e_2$, $\tau_o$, and $\varphi_o$. An expression for the sound velocity may be obtained from the equations of state by using the relation

$$c = \tau \sqrt{-\left(\frac{\partial \varphi}{\partial \tau}\right)_s} ,$$

which yields

$$c^2 = \varphi\tau \left( \frac{\left[\frac{Im}{kT} + \frac{5}{2}\right]^2 + \frac{5}{\alpha(1-\alpha)}}{\left[\frac{Im}{kT} + \frac{3}{2}\right]\left[\frac{Im}{kT} + \frac{5}{2}\right] - \frac{Im}{kT} + \frac{3}{\alpha(1-\alpha)}} \right) .$$

By the equations of state $c(\varphi, S)$ can be found in tabular form at least from

$c(\rho, \tau, T, \alpha)$ given above; likewise $\tau(\rho, S)$ can also be found so that the integral across the rarefaction wave leads to a tabulation of $u_{1r}$ as a function of $\rho_{1R}$ for values of $S_2$ and $\rho_2$ determined from the given $e_2$, $\tau_o$, and $\rho_o$. Another tabular function giving $u_{1s}$ in terms of $\rho_{1s}$ may be obtained from the shock conditions and the equation of state.

$$U/\tau_o = (U - u_{1s})/\tau_{1s}$$

$$\rho_{1s} + (U - u_{1s})^2 \tau_{1s} = \rho_o U^2/\tau_o$$

$$\tfrac{1}{2}(\rho_{1s} + \rho_o)(\tau_o - \tau_{1s}) = e(\tau_{1s}, \rho_{1s}) - e(\tau_o, \rho_o)$$

Here U, the shock velocity, and $\tau_{1s}$, the specific value behind the shock, must be eliminated in order to obtain the table.

The two tables, one giving $u_{1s}$ as a function of $\rho_{1s}$ and the other giving $u_{1R}$ as a function of $\rho_{1R}$ are used in conjunction with the contact surface conditions $u_1 = u_{1R} = u_{1s}$; $\rho_1 = \rho_{1R} = \rho_{1s}$ to obtain the desired expansion velocity $u_1$ for the specified $e_2$, $\rho_o$, and $\tau_o$.

A somewhat less general problem which may be solved in more detail is the one of finding the relationship of $u_1$ and $e_2$ knowing $\rho_o$, $\tau_o$ and imposing three plausible conditions on the flow that $\alpha = 1$ behind the contact surface, $\alpha = 0$ between the shock and contact surface, and $\frac{\rho_o \tau_o}{u^2} \ll 1$. The expansion at constant entropy can then be approximated by expansion with $\tau T^{3/2}$ constant since the assumption that $\alpha = 1$ before and after expansion means that the $\frac{I\alpha}{T}$ term in the entropy expression does not change much during the expansion.

Thus

$$u_{1R} = \int_{\rho_2}^{\rho_{1R}} \frac{\tau(\rho)\,d\rho}{c(\rho)}$$

reduces to

$$\sqrt{10(e_2 - I)} \cdot \left[1 - \left\{\frac{3\rho_{1R}\tau_o}{2\,e_2 - I}\right\}^{1/5}\right] .$$

Since $\frac{\rho_o \tau_o}{u^2} \ll 1$ we have for non-ionizing shocks in a monatomic gas

$$U = 4/3\ u_{1s} \qquad \text{(Eq. 69.01, Courant Friedricks)}$$

$$\rho_{1s} = 3/4\ \frac{U^2}{\gamma_0} \qquad \text{(Eq. 67.07, Courant Friedricks)}$$

From $\rho_1 = \rho_{1s} = \rho_{1R}$ and $u_{1s} = u_{1R} = u$, we obtain

$$u = \sqrt{10(e_2 - 1)}\left[1 - \frac{2}{e_2 - 1}\right]^{1/5},$$

or, letting $y = \frac{u}{\sqrt{e_2 - 1}}$,

$$(1 - \sqrt{.1y^2})^5 = 2y,$$

which has a solution $.32 < y < .24$

so that

$$u = .235\sqrt{e_2 - 1}\ .$$

If $e_2$ is considerably greater than I, the dependence of contact flow speed upon energy delivered to the tube is the one observed in Fig. 6. It is probable that this theory explains the relation observed in our early work, because in all likelihood the experimental curve is only an envelope of limited portions of the above equation in a variety of different gases, and the scatter of the experimental points has always been severe so that it was extremely difficult to draw a curve.

There is reasonably good agreement between the experimental slope of the curve in Fig. 6 and the theory above. The experimental slope of the most probable curve would lie somewhere between .09 and .12 $\frac{\text{cm/sec}}{\text{erg/gm}}$. The theoretical value is .14, based on an experimental efficiency of 50% in the transfer of energy from the capacitor to the discharge.

Present knowledge will not yet permit us to choose between two competitive theories for the production of luminosity, although experiments are in progress which are expected to provide this answer soon. The first theory is that the gas is excited to its highest temperature at the beginning of the expansion, and that thermal equilibrium prevails from then until the

end. The second theory is that the energy of the gas is initially stored in a few highly excited systems which are not in thermal equilibrium with the balance of the gas, and that the subsequent course of the expansion is a distribution of the energy of the few particles over the many in a general trend toward thermal equilibrium. Neither theory is completely in harmony with the experimental evidence, nor is the theoretical basis for one more completely acceptable than for the other.

The thermal equilibrium theory is countenanced by the experimental behavior of the multiple stages of ionization in elements like silicon, oxygen and carbon, and by the behavior of hydrogen as well. The achievement of maximum emission of each of these stages of ionization is highly suggestive of the Fowler-Milne theory of thermal radiation in stellar atmospheres. If correct, the belated rise to a maximum in the intensity of each spectral type is the be explained thus: Initially the gas is so hot that, due to electron and radiation impacts, the atom is never in its lower stages of ionization, and hence radiates little of these characteristic radiations. As the gas cools, there is a characteristic temperature at which each stage of ionization has a maximum population and a maximum radiation rate.

Statistical computations based on the non-equilibrium theory have never been satisfactory because the trend toward equilibrium always sets in too rapidly. Assuming that a few highly energetic ions and electrons accept the entire energy delivered to the tube, the time in which a $\frac{1}{e}$ portion of this energy would be spread over the entire assemblage is

$$\tau = \frac{1}{\sigma_i N v} \quad ,$$

where $\sigma_i$ is the ionization cross section, N is the number of neutral atoms per unit volume, and v is the electron velocity. To account for the measured power input (which largely precedes the rise of intensity of the discharge) at a level of only 1 to 10% initial ionization would require each particle to

carry $10^5$ - $10^6$ electron volts of energy. In this range $\sigma$ is known to be $\sim 5 \times 10^{-19}$ $cm^2$ and v is already near to the velocity of light. If N is about $10^{16}$ particles per cc as will be present at around 3 mm pressure, then $\tau$ is of the order of $3 \times 10^{-8}$ sec, far too short a time to account for the delayed intensity maximum. This is in accord with the well known fact that deviations from the Maxwell Boltzman distribution are very quickly suppressed by collision processes.

A computation of the speed of flow which would be expected from a given energy input fails either to give the observed dependence on the square root of the energy input per unit mass, or to account for the observed flow speeds within a factor of $10^3$ when the theory that there is small initial ionization is used.

The principal evidence in support of the non equilibrium theory is the space and time distribution of ion concentration which we, and Olsen and Huxford, have based on the assumed validity of the Holtsmark theory. These cannot be explained by a monotonically decaying ion concentration, but require an increase to a maximum before decay. The integrated exposure is also found to increase to a maximum, at very nearly the same time. If it be assumed that it is improper to apply the Holtsmark theory in the early stages of the expansion because the gas is too hot, then a correction factor for the Holtsmark ion concentrations, and the recombination coefficient which governs the luminosity, must show nearly identical dependence on ion temperature in order to give curves which have their maxima at the same point in time. The coincidence seems too remarkable to be accidental.

It is our tentative conclusion that the evidence favors the correctness of relative magnitude ion concentrations as calculated by the Holtsmark theory. The chief direct objection to using this theory is that it assumes a distribution of the surrounding ion cloud which should be static over

intervals of the order of the relaxation time of the atom, an assumption which is not completely justified by the facts. It has been customary to ignore the electron cloud which is present in the discharge plasma when making ion concentration estimates, on the assumption that it is not static, but rather averages to zero because of its rapid fluctuations. An estimate of the distance that a positive ion moves during atomic relaxation shows that it is not negligible, and hence casts doubt on the use of this theory. In addition, failure of the Holtsmark theory would give an elegant explanation of the belated rise to a maximum in time and space shown by the ion concentration curves. To the contrary, as we have already noted, it seems hardly credible that both the recombination coefficient and the Stark broadening should depend in the same fashion upon electron and ion temperature as would then be required to explain the agreement between the total intensity and squared ion concentration curves.

We therefore hold the view for the present that the passage of the discharge current stores energy in the gas in the main discharge section by imparting much energy to a few ions which then gradually share their energy with neutral atoms so that many ions are formed having little energy. Thus, the belated maxima arise from an ionization process which continues after the current subsides, essentially a thermal process.

A number of theories of the expanding luminosity have definitely been rejected in favor of the present theory. (1) The luminosity is not propagated by reabsorption of radiation, even though we recognize that radiation may act in several ways to produce secondary effects, i.e., the exterior gas may be preheated by radiation; the interior gas may lose energy more slowly because of its opacity to its own radiation; the apparent recombination coefficients may be reduced by reabsorption excitation. (2) The luminosity is not the result of an electron jet ejected from the

discharge. (3) The expansion is not the result of electrostatic repulsions set up in the discharge. (4) The energy which propels the expansion is not stored in the form of magnetic fields.

## CHAPTER V

## ENGINEERING APPLICATIONS

A number of aspects of the knowledge gained in this project have immediate engineering application. Recognition that shock processes are present has provided a new means of exciting strong shocks at low gas densities, for use in the investigation of high altitude behavior of airfoils. Shocks can be created in quick succession without the resetting of diaphragms necessary in conventional shock tubes. Manifold shocks can be made to pursue each other through the same gas, making possible a study of shock interactions. Apparent Mach numbers for shocks, referred to the undisturbed gas have been as high as 30. There is some reason to believe that these are only apparent numbers, since at these high flow speeds, the accompanying radiation probably preheats the undisturbed gas, so that it can only be said to be undisturbed in a mechanical sense.

A new principle of electronic switching using flowing ion clouds has been devised as a consequence of this work. The expanding ionized gas, including the shock itself when sufficiently ionized, may be used as a moving shorting bar to close a circuit between a pair of electrodes which remain inactive until the advent of the ion cloud. A number of such circuits can be closed in sequence at intervals as short as a fraction of a microsecond, the intervals being predetermined. Control over the time scale factor of the sequence of events can be had by external control of the speed of the ion cloud. By addition of sufficient energy to the gas at each extra electrode, the discharge might be made self-perpetuating. The device possesses considerable engineering potentialities.

It has been observed that any process which introduces disorganization

into the expansion promotes a more rapid decay of the luminosity, and probably of the ion concentration. It is likely that improved design of deionizing devices in circuit breakers may result from application of this new knowledge. On the same basis, abbreviation of photoflash discharges may be accomplished by suitable tube design.

# CHAPTER VI

## CONCLUSIONS

As a general theory of the Rayleigh phenomenon accompanying expanding spark discharges we propose that there are three phases to the life history of a spark discharge. (1) Breakdown of the dielectric. A voltage in excess of breakdown is abruptly applied to the electrodes. A luminous streamer of excitation traverses the tube from anode to cathode in $10^{-7}$ sec or less, propelled in all probability by the photoionization processes described by Loeb and Meek. We have observed this streamer and estimated its speed. This streamer discharges the interelectrode capacitor, and forms the region between electrodes into a plasma. (2) Discharge of the capacitor. A brief dark time sets in while the main discharge current is building up against the impedance offered by the circuit inductance. A current of 10,000 amperes peak value discharges the capacitor in about two to five microseconds (in our case). The discharge is brilliantly luminous. (3) Gas expansion. Coincident with this current, and lasting for an interval which may exceed it by a factor of as much as ten, an expansion of the hot, highly excited gas takes place. The expansion is preceded by a shock which is generally of sufficient strength to excite and ionize the gas it leaves behind. The shock is followed by an afterflow of products of the discharge which many lines of evidence indicate to be an active seat of exciting processes, probably electron collisions. The afterflow is brilliantly luminous. During all these processes the gas is believed to preserve a Maxwell-Boltzman distribution and the expansion is thought of as a succession of equilibrium states because the long range Coulomb forces between the ions promote rapid attainment of equilibrium. Conditions in the afterflow are highly suggestive of a stellar atmosphere.

## BIBLIOGRAPHY


1. V. Zahn, Wied. Am. 8: 675 (1879).
2. J. J. Thomson, Recent Researches in Electricity and Magnetism, Oxford, 115 (1893).
3. J. W. Beams, Phys. Rev. 36: 997 (1930).
4. L. B. Snoddy, J. R. Dietrich and J. W. Beams, Phys. Rev. 50: 469 (1936).

   L. B. Snoddy, J. R. Dietrich and J. W. Beams, Phys. Rev. 52: 739 (1937).
5. L. B. Loeb, Rev. Mod. Phys. 20: 151 (1948).
6. R. J. Strutt, Proc. Roy. Soc. 183: 26 (1944).
7. H. Zanstra, Proc. Roy. Soc. 186: 236 (1946).
8. R. J. Lee and R. G. Fowler, Phys. Rev. 81: 457 (1951).

   R. J. Lee, Thesis (M.S.), University of Oklahoma (1948).

   R. J. Lee, Proc. Okla. Acad. Sci. p. 62 (1948).
9. R. G. Fowler, J. S. Goldstein, and B. E. Clotfelter, Phys. Rev. 82: 879 (1951).

   B. E. Clotfelter, Thesis (M. S.), University of Oklahoma (1949).

   J. S. Goldstein, Thesis (M. S.), University of Oklahoma (1948)
10. W. Finkelnberg, Zeits f. Phys. 70: 151 (1931).

    W. Finkelnberg, Zeits f. Phys. Chemie B 11: 351 (1931).
11. R. V. Traubenberg, Phys. Zeits. 31: 958 (1930).
12. J. D. Craggs and W. Hopwood, Proc. Phys. Soc. 59: 755 (1947).
13. H. N. Olsen and W. S. Huxford, The Phys. Rev. 87: 992 (1952).
14. Summary Report, Dec.1951 Project No. NR 972-221/9-21-49,Contract No.N9 onr 97700.
15. H. E. Edgerton and P. M. Murphy, J. App. Phys., 12: 848 (1941).
16. H. N. Olsen and W. S. Huxford, J. of SMPTE 55: 285 (1950).
17. R. Courant and K.O. Friedrichs, Supersonic Flow and Shock Waves, Interscience, (1948).

Technical Report Distribution List

University of Oklahoma Research Institute

Contract No. N9-onr-97700

| Addressee | Attention | No. of Copies |
|---|---|---|
| Chief of Naval Research<br>Department of the Navy<br>Washington 25, D. C. | Code 427<br>Code 438<br>Code 421 | 5<br>1<br>1 |
| Director<br>Naval Research Laboratory<br>Washington, D. C. | Code 2000<br>Code 3320<br>Code 3150 | 9<br>1<br>1 |
| Chief, Bureau of Ships<br>Department of the Navy<br>Washington 25, D. C. | Code 816 | 2 |
| Chief, Bureau of Aeronautics<br>Department of the Navy<br>Washington 25, D. C. | Code EL | 1 |
| Chief, Bureau of Ordnance<br>Department of the Navy<br>Washington 25, D. C. | Re4f | 1 |
| Chief of Naval Operations<br>Department of the Navy<br>Washington 25, D. C. | Op 42 | 1 |
| Director<br>Naval Ordnance Laboratory<br>White Oaks, Maryland | Code 813 | 1 |
| Director<br>Naval Air Development Center<br>Johnsville, Pennsylvania | AEEL | 1 |
| Director<br>Naval Electronics Laboratory<br>San Diego, California | Technical Library | 1 |
| Director<br>ONR Special Devices Center<br>Port Washington, New York | | 1 |
| U. S. Naval Post Graduate School<br>Monterey, California | Electronics Engng.Dept. | 1 |
| Office of Naval Research Branch Office<br>150 Causeway Street<br>Boston 14, Massachusetts | | 1 |

| Addressee | Attention | No. of Copies |
|---|---|---|
| Office of Naval Research Branch Office<br>346 Broadway<br>New York, N. Y. | | 1 |
| Office of Naval Research Branch Office<br>844 North Rush Street<br>Chicago 11, Illinois | | 2 |
| Office of Naval Research Branch Office<br>1000 Geary Street<br>San Francisco 9, California | | 1 |
| Office of the Chief Signal Officer<br>Pentagon Bldg.<br>Washington 25, D. C. | SIGET | 1 |
| Signal Corps Engineering Labs<br>Evans Signal Laboratory<br>Fort Monmouth, New Jersey | Thermionics Branch | 1 |
| Research and Development Board<br>Pentagon Bldg.<br>Washington 25, D. C. | | 1 |
| Navy Research Section<br>Library of Congress<br>Washington, D. C. | | 2 |
| Mass. Inst. of Technology<br>Research Laboratory of Electronics<br>Cambridge, Massachusetts | Prof.A.Hill | 1 |
| Harvard University<br>Physics Department<br>Cambridge, Massachusetts | Prof. O. Oldenberg | 1 |
| Office of Naval Research Branch Office<br>1030 East Green Street<br>Pasadena 1, California | | 1 |
| Officer in Charge<br>Office of Naval Research<br>Navy #100, Fleet Post Office<br>New York, N.Y. | | 3 |
| Commanding General<br>Rome Air Development Center<br>Griffis Air Force Base<br>Rome, New York | RCRTM-1 | 1 |
| Northwestern University<br>Evanston, Illinois | Prof. W. T. Huxford | 1 |

| Addressee | Attention | No. of Copies |
|---|---|---|
| University of Michigan<br>Ann Arbor, Michigan | Prof. Otto Laporte | 1 |
| Commanding General<br>Air Force Cambridge Research Laboratory<br>230 Albany Street<br>Cambridge, Massachusetts | | 1 |
| Commanding General<br>Wright-Patterson Air Develop. Center<br>Dayton, Ohio | WCESD | 1 |
| University of Illinois<br>Department of Electrical Engineering<br>Urbana, Illinois | Prof. H. von Foerster | 1 |
| Stanford University<br>Department of Electrical Engineering<br>Stanford, California | Prof. I. Spangenberg | 1 |
| National Bureau of Standards<br>Central Radio Propagation Lab<br>Washington 25, D. C. | Electron Tube Lab | 1 |
| New York University<br>Physics Department<br>Washington Square<br>New York, N. Y. | Prof. M. Shamos | 1 |
| New York University<br>Physics Department<br>University Heights<br>New York 53, N. Y. | Prof. L. Fisher | 1 |
| University of California<br>Physics Department<br>Berkeley, California | Prof. L. B. Loeb | 1 |
| Johns Hopkins University<br>Physics Department<br>Baltimore, Maryland | Prof. G. H. Dieke | 1 |
| Tuskegee Institute<br>Tuskegee, Alabama | Dr. W. C. Curtis | 1 |
| Yale University<br>Physics Department<br>New Haven, Connecticut | Prof. H. Margenau | 1 |
| University of Southern California<br>Physics Department<br>University Park<br>Los Angeles 7, California | Prof. G. L. Weisler | 1 |

| Addressee | Attention | No. of Copies |
|---|---|---|
| Cornell Aeronautical Laboratory<br>4455 Genesee Street<br>Buffalo 21, N. Y. | Elma T. Evans | 1 |
| The James Forrestal Research Center<br>Princeton University<br>Princeton, New Jersey | Patricia Montenyohl | 1 |
| G-16, Littauer Center<br>Harvard University<br>Cambridge 38, Massachusetts | M.L. Cox | 1 |
| University of Toronto<br>Institute of Aerophysics<br>Toronto 5, Canada | R. Martino | 1 |
| National Sciences Foundation<br>Washington, D. C. | Dr. Raymond J. Seeger | 1 |